RI 9600

REPORT OF INVESTIGATIONS/1996

Application of Field Measurements and Computer Modeling To Evaluate Deep Mine Shaft Stability in Northern Idaho

UNITED STATES DEPARTMENT OF THE INTERIOR

UNITED STATES BUREAU OF MINES

U.S. Department of the Interior
Mission Statement

As the Nation's principal conservation agency, the Department of the Interior has responsibility for most of our nationally-owned public lands and natural resources. This includes fostering sound use of our land and water resources; protecting our fish, wildlife, and biological diversity; preserving the environmental and cultural values of our national parks and historical places; and providing for the enjoyment of life through outdoor recreation. The Department assesses our energy and mineral resources and works to ensure that their development is in the best interests of all our people by encouraging stewardship and citizen participation in their care. The Department also has a major responsibility for American Indian reservation communities and for people who live in island territories under U.S. administration.

Report of Investigations 9600

Application of Field Measurements and Computer Modeling To Evaluate Deep Mine Shaft Stability in Northern Idaho

By M. J. Beus, T. J. Orr, and J. K. Whyatt

UNITED STATES DEPARTMENT OF THE INTERIOR
Bruce Babbitt, Secretary

BUREAU OF MINES
Rhea Lydia Graham, Director

International Standard Serial Number
ISSN 1066-5552

CONTENTS

ILLUSTRATIONS

TABLES

UNIT OF MEASURE ABBREVIATIONS USED IN THIS REPORT

Metric Units

cm	centimeter	m^3	cubic meter
GPa	gigapascal	Mbyte	megabyte
h	hour	mm	millimeter
Hz	hertz	MPa	megapascal
km	kilometer	N	newton
km^2	square kilometer	t	metric ton
kN	kilonewton	°C	degree Celsius
m	meter		

U.S. Customary Units

ft	foot	mi^2	square mile
ft^3	square foot	psi	pound per square inch
in	inch	st	short ton
lb	pound	°F	degree Fahrenheit

Reference to specific products does not imply endorsement by the U.S. Bureau of Mines.

Disclaimer of Liability

The U.S. Bureau of Mines expressly declares that there are no warranties expressed or implied that apply to the software described herein. By acceptance and use of said software, which is conveyed to the user without consideration by the Bureau of Mines, the user hereof expressly waives any and all claims for damage and/or suits for or by reason of personal injury, or property damage, including special, consequential, or other similar damages arising out of or in any way connected with the use of the software described herein.

APPLICATION OF FIELD MEASUREMENTS AND COMPUTER MODELING TO EVALUATE DEEP MINE SHAFT STABILITY IN NORTHERN IDAHO

By M. J. Beus,[1] T. J. Orr,[2] and J. K. Whyatt[1]

ABSTRACT

Researchers at the U.S. Bureau of Mines have developed personal-computer-based data acquisition, instrumentation, and mine visualization and modeling techniques to evaluate a mine accessway in a deep hard-rock mine in northern Idaho. These techniques were applied to a mine shaft in a large silver mine that has been in operation for many years. A very deep, rectangular, timber-supported shaft extending to depths exceeding 2.3 km (7,500 ft) had been deforming continuously as a result of nearby mining, resulting in operational problems. Preliminary visual observations and rock and support monitoring confirmed that severe diagonal distortion was occurring. Extensive field measurements and data analysis confirmed initial observations, provided insights into the cause of deformation, and defined a general approach to structural modeling.

Computer analysis of the problem was initiated by developing a three-dimensional model of the terrain. This represented a volume of rock approximately 80 km^3 (40×10^{10} ft^3) and an area on the surface surrounding the mine 9 km^2 (3 square miles). Based on this model, a three-dimensional, finite-element analysis was conducted to establish boundary conditions for sequentially more detailed two- and three-dimensional submodels of the shaft area. Results from the computer study are being used to develop new approaches to mine design and to provide design guidelines for deep mine accessways subject to severe rock-mass loading conditions.

[1]Mining engineer.
[2]Mechanical engineer.
Spokane Research Center, U.S. Bureau of Mines, Spokane, WA.

INTRODUCTION

Some of the deepest mines on the North American continent continue to be important sources of base metals, such as antimony, silver, copper, lead, and zinc. Despite intense global competition and increasingly stringent environmental regulations, existing deep mining operations remain profitable. Application of advanced technology to enhance safety and productivity in deep mine accessways is important to this success.

The most important of all deep mine openings is the shaft. Shafts are the lifeline of the mine and must be well designed and maintained to provide for a long service life. This is particularly important if the shaft is highly stressed and close to mining. In many cases during shaft operations, ground control is not a problem, and shaft monitoring is conducted solely for the purpose of hoisting safety and operational efficiency. However, instabilities can develop as a result of several factors, including nearby mining, development of auxiliary openings such as loading pockets and stations, squeezing ground, and rock bursting. Figure 1 shows collapse of a shaft support structure that could have resulted from instability in the rock mass.

Previous research by the U.S. Bureau of Mines (USBM) has investigated various approaches to shaft design and monitoring, including structural analysis to validate, modify, and refine design parameters before, during, and after a shaft was constructed (*1-3*). These parameters included size and shape of the opening, artificial support requirements, and optimum orientation of the shaft with respect to principal rock forces and geologic discontinuities.

Many researchers have investigated these problems in order to develop optimum shaft pillar dimensions and support strategies (*4-8*). For the present work, an integrated approach is suggested in which many of the research accomplishments from previous investigations are combined with applications of new technology. This study describes computer visualization, analysis, and rock mass monitoring of a shaft while in service. The study includes the use of advanced computer technology to simulate the complex geometric configurations and displacement trends of a rock mass and mine openings, real-time data acquisition from rock mechanics instruments, and new innovations in measuring rock-mass displacement.

This research was conducted in the No. 10 shaft in the Sunshine Mine in the Coeur d'Alene Mining District of northern Idaho. Figure 2 shows the location of the shaft at the Sunshine Mine. This is a deep rectangular shaft that has been in service for many years and was undergoing severe distortion as a result of nearby mining and ore pass construction. The squeezing nature of the rock mass and the presence of rock-burst-prone areas in the shaft pillar further complicated the situation. This shaft is a crucial accessway that must be maintained for ventilation and escapeway purposes, as well as for production. Maintenance and guide realignment were major mining costs and significantly affected the overall economics of the operation. In addition, the shaft area in this particular section of the mine contains significant quantities of silver, copper, and antimony. Monitoring and analysis of the shaft would enable mine operators to assess its structural integrity and stability and permit the possible recovery of these valuable resources. Figure 3 shows the guides and shaft sets in the "chippy," or manway, compartment of the shaft, where preliminary observations were conducted.

Major tasks for this work included (1) definition of the deformation and loads acting on the rock mass and shaft support system, (2) determination of the physical properties and strengths of the rock mass, (3) definition of the geometry of the shaft and surrounding mine openings, (4) simulation of the geometry and removal of the rock mass, and (5) definition, analysis, and validation of structural behavior at the scale of interest. The present study uses personal-computer (PC-) based two- and three-dimensional visualization and structural analysis that takes into account topography, gross geologic features, and detailed mine opening and support geometry. Field measurements are used to analyze the cause of shaft deformation and to confirm the structural analysis.

FIELD STUDY

MONITORING SYSTEM

The major components required for the mine monitoring system are sensors, data acquisition system (DAS), and processing hardware and software. Previous mine monitoring and process control systems have often not met the requirements of cost effectiveness, sensor diversity, and the simplicity and ruggedness that would allow the system to withstand the rigors of long-term, unattended underground operation.

Based on many years of in-mine testing and experience (*9*), the USBM has developed cost-effective mine-ready

sensors and computerized data systems for coal and metal mines.[3] These processors and DAS's are packaged for protection from the harsh mine environment. A "factory floor" PC in a NEMA IV box has been adapted for use underground. The present configuration is a passive backplane system with a board-level processor mounted in a stainless-steel box that contains an air-to-air heat exchanger (figure 4).

Rock mass and mine environment sensors are connected to what are called "isolated measurement pods" or IMP's (*10*). This system can provide input-output (I/O), signal conditioning, and analog-to-digital conversion for up to 600 channels on one interface card with a scan rate of 1 Hz for a wide variety of sensors. The IMP's are inherently protected from the environment and require no further packaging, although they often are stacked in a larger enclosure with a power supply and connector blocks. The network (S-Net) can extend in a parallel configuration up to 1 km (0.6 mile) in either direction from the PC and the distance increased in 1-km increments using S-Net repeaters.

Research has also been directed toward developing and testing procedures for processing and visualizing output from ground-condition sensors in "real time." Real time has been defined in a broad sense as the amount of time sufficient to make decisions. For example, by monitoring ground movement and liner loads during shaft sinking, design decisions can be made daily, and even hourly, by construction supervisors. Real-time monitoring of ground response to actual mining and natural forces, such as high stress, can vary from seconds to days or even years. In deep mines experiencing heavy ground and rock creep, data must be accumulated and assessed over long periods in order to develop and verify designs or activate ground-control measures. Ground-control decisions depend on the scope of the process being monitored, and the time available to make these decisions can vary from a few milliseconds in the case of rock bursts to days or weeks for long-term creep.

Software

The key to real-time operation for operator interface and visualization is the processing and communication software. In this study, PC-based software was used exclusively because of its availability and the existence of a large, experienced user base. Applications work in background and foreground and as subroutines to general-purpose communication and spreadsheet programs. The core of the software is a real-time monitor (RTM) (*10*). The RTM allows data to be displayed in a variety of formats, including row-by-column spreadsheets, bar graphs, trend graphs, and alarm summaries. The coprocessor can be left operating in the background, which permits other programs, such as communications or plotting packages, to be operated in the foreground. This program is left in host mode waiting for an incoming call from a remote computer to download data files. Communication is via shorthaul modems to the surface and high-speed (9600-baud) modems to remote terminals. Figure 5 shows the layout of this system at the Sunshine Mine.

Sensors

The second major component of the mine monitoring system is the in-mine sensors. Sensors must survive the unusually hazardous conditions of underground operations, including hot, humid, and corrosive atmospheres; water and falling rock and debris; and shock loads from blasting. Most importantly, the system must be cheap, simple and fast to install, and durable over long periods of time. Sensors have been selected and repackaged to survive these underground conditions and mining operations.

Monitoring of rock movement forms the backbone of the geosensing ground-control network. The current design favors linear or string potentiometers (SP's) linked to multiple, individually anchored sensing positions distributed down the length of a borehole. A mechanically anchored mounting head that provides for in-hole adjustment to accommodate an infinite range of rock movement has been tested. The head is recoverable upon completion or abandonment of the site. It may also be fitted with an accelerometer that will trigger data scans concurrently with blasting. Other basic ground-condition sensors used during this project include USBM-developed timber and bolt load cells, SP's for measurements of structural deformation on shaft sets, and temperature detectors.

SHAFT AND STATION INSTRUMENTATION

Preliminary Data

Preliminary observations and tape extensometer displacement measurements were taken on six shaft sets across the chippy compartment in the vicinity of the 4300 level of the mine. Measurements in the east-west and north-south directions confirmed that diagonal distortion across the shaft opening was occurring even though there was no mining in this area. Figure 6 shows the diagonal distortion in shaft support sets measured in sets 40-16 through 46-15 from about the 1,370- to the 1,570-m (4,100- to 4,700-ft) depths. In general, the east-west diagonals are

[3]The results of one such project will be published during 1995 in a USBM RI entitled "Real-Time Monitoring of Field Measurements for Mine Design: Greens Creek Mine, Admiralty Island, AK," by T. J. Orr and M. J. Beus.

lengthening (positive movement) and the north-south diagonals are shortening (negative movement). The north-south shortening is considerably greater than the east-west lengthening. The maximum amount of distortion [18 mm (0.7 in) at a rate of about 2.53 mm/month (0.1 in/month)] is centered around set 42-14 just above the 4300 level.

Three-dimensional plots of the diagonal displacement data are shown in figure 7. Distortion is clearly concentrated at a particular depth in the shaft. Figure 7*A* indicates that change in north-south displacement is greatest between the 4200 and 4400 stations at 1,400 and 1,466 m (4,200 and 4,400 ft), respectively, and tails off above the 4000 and below the 4600 levels at 1,333 and 1,533 m (4,000 and 4,600 ft), respectively. Figure 7*B* shows the east-west displacement maximum at about the 4400 level. Even though these three-dimensional surfaces are based on a small number of data points, the trends seem to be consistent and would indicate that the planned shaft instruments should be located between the 4200 and 4400 levels to obtain the most information.

A more detailed analysis indicates possible factors causing this distortion pattern. Figure 8 shows a localized shear mechanism that could account for the distortion. The rock mass appears to be slumping into the mined-out stope (South Split of the Chester vein) located southwest and down-dip of the instrumented shaft interval. This movement likely reflects some combination of an optimal position in the strata with respect to mining and/or the presence of a fault or set of soft, weak strata that results in a concentrated shear deformation.

This shaft section lies within a moderately thick [61 m (200 ft)] set of relatively soft, overturned siltite-argillite beds. These strata underlie a thick [122 m (400 ft)] interval of overturned, strong vitreous quartzite beds. Immediately below the siltite-argillite beds is a thin [30 m (100 ft)] interval of strong sericitic quartzite. This sequence results in an unusual instance when rock mass deformation may actually *increase* a shaft dimension, producing an effect observed by the measured shaft deformation pattern. In fact, this lengthening cannot occur without a *local* amplification of distortion like that indicated by the chippy compartment measurements.

Field Installation

On the basis of preliminary data, a comprehensive sensor array was installed in the shaft and at the station on the 4400 level. Multiple-position borehole extensometers (MPBX's) were installed on the 4400 level in four boreholes and designated E1, E2, E3, and E4 (figure 9). The location, orientation, depth, and size of installation holes into the rock mass were predetermined on the basis of geology and preliminary structural analyses. Displacement anchor positions were predetermined at five locations in each borehole. Three 3.8-cm (1.5-in) diam holes were drilled approximately 46 m (150 ft) northeast of the shaft to an approximate depth of 17 m (55 ft) with a 7.6-cm (3-in) collar section. E1 was aligned parallel to bedding, E2 was aligned 45° to bedding, and E3 was aligned normal to bedding. E4 was drilled southwest of the shaft to approximately 23 m (75 ft) and aligned parallel with the Chester vein and bedding.

A platinum resistance temperature detector (PRT) was installed in the collar of E1 to provide a temperature history at this location. A temperature profile on E1 was also compiled prior to installation of the MPBX to determine if a temperature correction would be required on the downhole instruments. A comparison indicated about a 5 °C (10 °F) difference between the collar and the rock at the 17-m (55-ft) depth. This is not a large enough difference to affect the MPBX's, particularly using the fiberglass rod anchor extensions.

Additional instruments were installed in the timber shaft set at the 4300 level and included load cells (LC's) to monitor timber set loads at each blocking point and SP's to measure set distortion and rotation (figure 10). Two single-point extensometers (SPBX's) monitored closure between the shaft set and the south shaft walls. A PRT monitored temperature within the compartment. All instrument data were collected three times daily through the DAS in the No. 10 shaft hoist room on the 3700 level, 1,773 m (5,200 ft) below the surface. A precision reference resistor with a tolerance within ±0.001 ohm was used to evaluate the stability of the system.

Data Analysis

Figure 11 shows initial time plots of the MPBX's on the 4400 level near the shaft. Deformation rates indicate the outstanding precision of the MPBX's, but precision may be outstripping accuracy. That is, the trends are likely to be significant, but the magnitudes measured by different channels may be of the same order as differences in systematic errors (rod friction, potentiometer characteristics, borehole deterioration, etc.).

The MPBX's, after "bedding in," indicated a trend toward long-term rock creep. The results shown are net displacements of each individual anchor with respect to the deep anchor, 17 m (55 ft) for E1, E2, and E3, and 23 m (75 ft) for E4. At first, E1 showed a negative displacement of the borehole collar and the 7-m (20-ft) anchor of about 0.4 mm/month (0.015 in/month). The deep anchors of E1 were essentially not moving beyond the overall

resolution of the DAS of ±0.1 mm (±0.005 in). About 3 months after installation, the collar and the 7-m (20-ft) anchor began to close, reversing the trend, possibly in response to work on the shaft that was initiated about this time. E1 continued to indicate extensional creep of the borehole collar of about 0.05 mm/month (0.002 in/month), up until the time the system was disconnected at day 250. E2, E3, and E4 maintained a general trend toward extensional creep, or lengthening of the borehole between the collar and the remaining anchors. The apparent creep rates of E2 and E3 were roughly equivalent at a constant 0.2 mm/month (0.006 in/month). E4, parallel to the vein but closer to the shaft, recorded about three times that rate at 0.5 mm/month (0.018 in/month), with the 3-, 7-, 9-, 15-m (10-, 20-, 30- and 50-ft) positions similar for the first 100 days and then reversing.

It is informative to look at individual anchor displacements, rather than differences in displacement as plotted in figure 11. The incremental displacements indicated by each MPBX over 50-day monitoring periods are shown in figure 12. E1 shows a consistent change from shortening of the borehole in the first two periods to lengthening in the last three periods. This shortening suggests some change in the driving mechanism late in the 50- to 100-day interval. The lack of significant response by the 7-m (20-ft) anchor, despite similar responses from the 3- and 9-m (10- and 30-ft) anchors, suggests that the 7-m (20-ft) anchor malfunctioned. It is very unlikely that shortening and lengthening of the borehole is occurring in equal amounts within 3 m (10 ft) on each side of the 7-m (20-ft) anchor. The similar displacement rates measured by the remaining channels suggest deformation is concentrated in the first 3 m (10 ft) of the borehole.

E2 shows a consistent rate of lengthening throughout the entire monitoring period. The change in behavior noted in E1 is not evident here. The displacement pattern does resemble that for E1, however, in suggesting that rock deformation is concentrated in the first 3 m (10 ft) of the borehole.

E3 shows a more chaotic picture, although there is consistent lengthening of the borehole measured on all channels. Any change in behavior correlating with that observed in E1 is lost in the measurement noise. The chaotic pattern prevents any conclusion as to the relative location of the deformation, although lengthening in the first 3 m (10 ft) of the borehole would be consistent with the measurements.

E4, south of the shaft, was probably placed in the softer, overturned siltite-argillite near the top of the vitreous quartzite unit. The displacements measured on the various MPBX channels are up to an order of magnitude larger than those measured in the sericitic quartzite north of the shaft. Relative creep rates are consistent with earlier measurements. Also, there is a clear change in displacement rate starting late in the 50- to 100-day period, as indicated by E1. Unlike at E1, however, this change is reversed and later periods (between 150 and 200 days, and 200 and 250 days) show a drift back toward initial rates.

The orientations of E1, E2, and E3 are also suggestive of orthogonal components of a vector. While this is not exactly true (the angle between E1 and E3 is 60° and the other angles are 98°), the displacements and orientation can be combined to calculate a total displacement vector. In this case, the relative displacement of the collar with regard to the deepest anchor is assumed to be the best measure of rock displacement. Table 1 shows estimates of displacement magnitude and direction derived for each 50-day period, as well as total magnitude and average bearing and plunge for the entire monitoring period. The initial 0- to 50-day vector points downward and west, but rotates toward deeper mining to the southwest over the entire 0- to 250-day period.

Assuming that the initial deformation rate is valid, a review of changes in the deformation vector also produces interesting results. That is, assuming the 0- to 50-day rate is a steady-state background deformation rate, a vector representing the change in displacement can be calculated. Adding this vector to the 0- to 50-day vector will produce the original vector for that period. The results are given in table 2.

Table 1.—Rock displacement vector by monitoring period

Days elapsed	Magnitude	Bearing	Plunge
0-50	0.0316	S 84° W	31°
50-100	0.0220	S 68° W	33°
100-150	0.0169	S 23° W	25°
150-200	0.0186	S 28° W	24°
200-250	0.0260	S 49° W	29°
0-250	0.1072	S 52° W	29°

Table 2.—Incremental displacement vector

Days elapsed	Magnitude	Bearing	Plunge
50-100	0.0116	S 68° E	-21°
100-150	0.0255	S 62° E	-21°
150-200	0.0240	S 58° E	-21°
200-250	0.0200	S 36° E	-20°

NOTE.—The assumption is that the 0- to 50-day vector represents the background creep rate.

These displacement vectors indicate that the borehole collar is moving westward, presumably taking on extra load from buckling of the weak strata in the J-vein footwall. Subsequent mining in the Chester stopes may have exerted

an incremental pull on the borehole collar, rotating the total displacement vector to the southwest. This explanation is consistent with the change in character observed in two of the four MPBX's.

The 12 LC's in the timber set at the 4300 level monitored normal loads in the set members (figure 13). The LC's were blocked in to a preset load up to approximately 11×10^3 N ($(25 \times 10^3$ lb) (figure 12*A*). In figure 13*B*, the divider loads were not uniform because of interaction with adjacent sets and the complex behavior of set member joints. The end plates and wall plates (shown as 14, 10, 7, 11, 18, 15, 12, and 3 in figure 10) exhibited generally higher loads, probably because of direct loading from the hydraulic jacks used to move the set into proper alignment. Most of the LC's shown in figure 13*A* showed increasingly uniform loads slightly greater than the initial blocking-in loads, up to a maximum of about 13.6×10^3 N (30×10^3 lb), with the exception of LC 15. LC 3 and LC 10, and LC 12 and LC 14 on opposite ends of the wall plates were grouped in the same general load range and reflected an approximately equal load.

Loads were generally higher on the end plates, as indicated by LC 18 and LC 15, and LC 7 and LC 11. The LC's across the dividers in figure 13*B* (LC 9, LC 13, LC 16, and LC 17) generally reflected a smooth transfer of end load across the member, particularly the divider between the skip compartments (LC 9 and LC 17). Loads were roughly equal in magnitude, with the exception of the load on LC 16, which malfunctioned. All LC's appear to have lost load from the blocking-in, probably because of jacking on the end and wall plates, and subsequent excessive squeezing around the blocking point along the long sides of the shaft wall across the dividers. The general lack of agreement between loads on opposite ends of the same set members is somewhat surprising. This result might be explained by set distortion caused by interaction with adjacent sets above and below and the dividers between compartments, which may have prevented a smooth transfer of axial load through the members.

Initial and final loads show that the end wall LC's maintained minimal loads, probably as a result of the fractured rock zone that developed parallel to bedding strike in the shaft end walls. The sidewall LC's, on the other hand, recorded a marked north-south variation. The most northerly LC's initially recorded high loads that gradually decreased over time, while the most southerly LC's initially recorded little load that gradually increased over time. The intermediate LC's on each wall provided intermediate load histories.

Initial loading of the timber set was almost entirely by normal loading at the blocking points. Shear loads may develop with time, but these will likely develop primarily in opposition to set distortion resulting from imbalances in the applied normal loads. The distortional forces on the set can be analyzed by simple moment-and-force balance. The initial loads show that the rock exerted a counterclockwise torque and a westward push on the set. The velocity of set distortion is low, so frictional forces must develop to oppose these forces. The set distortions measured by the SP's and preliminary measurements in the chippy compartment are consistent with this loading. The final loads show similar but increased levels of both torque and westward push.

SP's provided extremely good data, in spite of the exposure of the sensing wire to the shaft environment. Figure 14 shows the diagonal distortion of the three shaft sets centered at the 4300 level. The plots in figure 14*A* spanned the outside of three sets diagonally on the north and south ends, and the plots in 14*B* spanned the front (west) side of the shaft. (The LC's are on the middle set at the 4300 level.) Note the equal and opposite response, that is, one diagonal shortened as the other lengthened at a rate of about 0.8 mm/month (0.03 in/month) on the ends of the set. SP 1 apparently malfunctioned around 100 days after installation.

The diagonal displacement on the front of the shaft (figure 14*B*) is about five times the magnitude of the measurements on the ends, indicating excessive end plate squeeze (see loads on end plate LC's 7, 11, 18, and 15 in figure 13). The diagonal distortion across the back of the shaft at SP 3 and SP 4 is about one-third that on the front. Figure 14*C* shows movement from the short diagonals and north and south ends of the shaft at the center shaft set on the 4300 level. All these indications point to significant distortion and squeezing (shortening) at the end of the shaft.

The SP plots show the same diagonal deformation pattern observed in the chippy compartment and suggest a complex, three-dimensional distortion of the shaft timbers. A simplified view of these measurements assumes that all displacements occurred as horizontal deformation of the bottom set with respect to the top set. The north-south deformation components showed torsion of the shaft set consistent with observations in the chippy compartment. In addition, east-west deformation components estimated from end wall deformation suggest that the south end of the set is moving westward as well. Conversely, all deformation can be assumed to be vertical. In this case, the southwest corner is moving downward while the northwest and southeast corners are moving mainly upward. Again, the northeast corner appears to be relatively static.

Temperatures at E1 on the 4400-level drift (figure 15*A*) are relatively stable, around 27 to 28 °C (80 to 85 °F). Figure 15*B* shows the shaft temperature inside the chippy compartment and reflects seasonal changes.

COMPUTER ANALYSIS

The approach to pc-based computer modeling was to employ "submodeling" for an analysis of the specific mining features within the large rock mass surrounding the No. 10 shaft. This technique allows target features to be remodeled using results from a "supermodel." Submodels are developed in ever-increasing detail, or nested, until the desired level of detail is obtained (*11*). A series of nested submodels were used to determine the detailed structural response of the various mine openings and support structure to nearby mining. Table 3 shows pertinent modeling statistics.

The initial model contained a surface area of 9 km^2 (3 square miles) around the No. 10 shaft. The scale of the topographic model prohibited direct modeling of the shaft and nearby mining. Detailed analysis required a stress surcharge on the initial submodel boundaries based on previous data. The three-dimensional topographic supermodel represented a volume of rock approximately 80 km^3 (40×10^{10} ft^3) and established the boundary conditions for subsequently more-detailed submodels. A smaller model about 2,000 m (6,000 ft) on a side provided some detail of the Chester vein footwall, South Split vein, and J vein using boundary conditions derived from the topographic model. Submodels 400 m (1,200 ft) on a side provided better detail of the three main mined-out stopes that seemed to be redistributing load around the No. 10 shaft near the 4400 level. The scale on the detailed vein models still proved to be too large to allow direct modeling of the No. 10 shaft or the surrounding openings. Therefore, small-scale submodels were constructed using boundary conditions from the detailed vein models. Models of the motor barn instrumentation area, the No. 10 shaft 4400 station, and the shaft set on the 4300 level were used to evaluate sensor data.

REGIONAL STRESS FIELD

A regional analysis of the stress field was conducted to evaluate in situ stress fields that had been determined from field measurements and observations of failure patterns. The stresses acting on the rock mass at the Sunshine Mine consist primarily of gravitational and tectonic forces. Typically, gravitational stress is estimated by a simple depth-of-overburden calculation based on the density of the overlying material. While this estimate is suitable for flat-lying, shallow deposits under gentle topography, field stresses in the Sunshine Mine are affected by nonuniform distribution of gravitational forces from the mountainous terrain and tectonic forces.

Figure 16 shows a computer-generated view of the topography around the Sunshine Mine and includes the surface over an area of 28 km^2 (9 square miles) centered around the mine. This area simulates a block of ground approximately 5,333 m (16,000 ft) on a side centered around the No. 10 shaft and extends from the surface near Polaris Peak [1,567 m (4,700 ft) in elevation] to a depth of about 1,667 m (5,000 ft) below sea level. The surrounding topography of the surface was digitized from a U.S. Geological Survey topographic map of the vicinity. A three-dimensional surface mapping program called Surfer was used to generate the topographic model. Randomly spaced elevations were selected to define mountain peaks and stream beds.

The topographic program filled in a uniform grid of approximately 1,000 elevation data points with evenly spaced x and y coordinates. The data were input into the AutoCAD computer program for visualization purposes, and x, y, z data were converted into finite-element key point and volume commands. All materials in the block were assumed to behave elastically. Roller boundary conditions were established on all cut boundaries, and a vertical gravity load was applied. The model served to estimate in situ stress and generate boundary conditions for subsequent submodels. The computed magnitude of vertical stress agreed well with what had been previously determined. The ratio and direction of horizontal stresses also agreed well with what had been measured previously, but the magnitude was significantly less.

Table 3.—Modeling statistics for deep mine supermodels and submodels

Description	Size		ANSYS element type	Wave-front RMS/max	Element/ nodes	486 run time, h	File size, Mbyte
	meters	feet					
Topographic stress	4,877	16,000	Stif 45 brick	799/?	7200/8649	20	311
Gross vein	1,829	6,000	Stif 92 tetra	897/?	3403/3403	10	126
Detailed vein	366	1,200	Stif 45 tetra	662/1048	7308/1352	4	180
4400 station	46	150	Stif 45 brick	893/1234	4750/5952	29	207
Motor barn MPBX site	30	100	Stif 45 brick	955/1047	4200/4928	29	194
4400 level[1]	366	1,200	Stif 42 quad/tri	206/?	2693/2637	0.66	16
4300 shaft set[1]	46	150	Stif 42 quad/tri	161/?	1913/1740	1	25

[1]Two-dimensional.

Figure 17 shows the vertical stress distribution on a horizontal slice at the 4400 level 1 km^2 (0.6 square mile) in area centered around the No. 10 shaft where north is at the top of the figure. Vertical stress increases linearly with depth throughout the test area to approximately 46 MPa (6,500 psi) at the 4400 level. Stress increases in intensity toward the southeast. Horizontal stress at the 4400 level, which is under about 533 m (1,600 ft) of overburden, is 62 MPa (8,800 psi) maximum at N 70° W, aligned with the short axis of the shaft, and 35 MPa (5,000 psi) minimum.

SUBMODELING

A three-dimensional, computer-aided design (CAD) drawing of the vein geometry surrounding the No. 10 shaft from the 4000 level to the 4600 level was compiled from company drawing files. Ore deposits, mined and backfilled areas, reserves, and major geologic features are shown in figure 18. A complicating factor was the mix of intact ore material, mined-out areas left open, and mined-out areas that had been backfilled, which resulted in a situation where various material types and physical properties had to be taken into account. Physical properties used for the intact rock assumed that modulus of elasticity varied by a factor of two and was a function of bedding orientation. Bedding in this vicinity strikes approximately parallel with the long axis of the shaft. Moduli of deformation of 21 and 10.5 GPa (3×10^6 and 1.5×10^6 psi) were used for the host rock quartzite in directions parallel and perpendicular to bedding, respectively. Vein material was assumed to have the same stiffness as the cross-bedded quartzite.

A gross vein submodel was then used to represent a volume of rock 2,000 m (6,000 ft) on a side. However, a smaller submodel obtained better detail of the three main mined-out stopes, which seem to be redistributing the load on the shaft sets. This model includes a block of ground approximately 400 m (1,200 ft) on a side centered around the No. 10 shaft at the 4400 level; boundary conditions were calculated from the gross vein submodel. Figure 19 shows this model with the 4400 station and motor barn MPBX site submodels inside.

The motor barn and shaft submodels include a block of ground about 46 m (150 ft) on a side extending from the 4000 level to the 4400 level. The development openings, including the shaft and adjacent drifts and cross-cuts, are characterized as smooth, rectangular shapes. Stopes are represented by three separate cavities 122 to 183 m (400 to 600 ft) long, 3 m (10 ft) wide, and 61 to 122 m (200 to 400 ft) deep.

These submodels required two load steps to determine the effect of nearby mining on the openings. The first load step simulated premining conditions. Boundary conditions for the first load step were obtained from the detailed vein model, which enveloped all submodels and had loading surfaces oriented along principal stress directions. The second load step, representing a single mining step in which all the ore was removed at once, established postmining boundary conditions and results. The premining load step was subtracted from the postmining load step to get the net effect of mining in the area of interest. This simplification required that the veins be analyzed as having a constant dip angle over some distance, a constant thickness with no undulations in the plane of the vein, and constant material properties. The different orientations of each void caused considerable difficulty in obtaining an adequate mesh.

The scale was still too coarse to allow detailed modeling of the No. 10 shaft and surrounding openings. Therefore, the final two models were two dimensional (based on the previous submodels) and simulated the effects of past mining of the J vein and the South Split vein of the Chester vein. There were no rock bolts used in this analysis. The intent was to verify the out-of-squareness of the shaft cross section and the shaft set. This was determined by simulating the approach of mining from the J vein and the South Split vein. Figure 20 shows the two-dimensional, cross-sectional mesh developed to show these veins in relation to the No. 10 shaft. In figure 20*A*, the South Split vein of the Chester vein approaches the shaft from the south at a small angle to the shaft's long dimension. Stoping occurs in a single cut to within about 30 m (100 ft) of the shaft. A mesh was made in which the shaft was considered to be a rectangular rock section with dimensions of 3 by 9 m (10 by 30 ft) in full section, as shown in figure 20*B*. Figure 20*C* shows the shaft set mesh at the 4300 level.

RESULTS

Computer modeling delineated areas of extensive movement toward the shaft from the mined areas and differential displacements around the shaft. Preliminary comparisons with shaft excavation and set distortion and shaft pillar displacement indicate that the trend of observed movement is in general agreement with the results of the analysis. For example, it was observed that the north side of the 4400 station excavation servicing the shaft was deforming vertically upward with respect to the south side, and that there was a resultant shortening of the north-south diagonal and a lengthening of the east-west diagonal in the compartments. This observation was confirmed by the measurements taken. Figure 21 shows the relative difference in vertical deformation of the rock mass between the northwest and southeast corners of the shaft opening. The rock mass surrounding the southeast corner

deflects downward over 12.7 cm (5 in) with respect to the rock mass in the northwest corner.

Figure 22 shows the maximum stress surrounding the shaft section. Premining values of compression range from about 7 MPa (1,000 psi) at the midpoint of the long axis to over 154 MPa (22,000 psi) near the yield point at the northeast and southwest corners (figure 22*A*). There is a significant increase in stress levels at the northeast and southwest corners as mining proceeds. Figure 22*B* shows the shaft corner stress after the South Split vein on the Chester vein is "mined" and corner stress exceeds the yield point.

Figure 23 shows the rotational trend and translation of the chippy compartment in the shaft support set. The displacement contours in figure 23*A* show north-south movement and indicate a translation toward the north (the darker shades indicate greater movement). This result is compatible with the findings from the shaft cross-section model. Figure 23*B* shows east-west movement, indicating a lengthening of the east-west axis and extensive translation toward the east. The entire section is translated toward the northeast ore pass with the southeast corner moving a greater distance than the northwest corner, as indicated by the length of the displacement vectors. This displacement would tend to rotate the section counterclockwise, shortening the north-south axis and lengthening the east-west axis. This finding is consistent with the diagonal measurements in this vicinity of the shaft. The general trend of the computed diagonal displacements is in good agreement with observed and measured deformation in the No. 10 shaft sets.

CONCLUSIONS

On the basis of field measurements, mining of the J vein below the 4400 level near the No. 10 shaft is considered to be the predominant mechanism for shaft deformation. Interaction of the mining pattern with variations in rock strata created localized zones of amplified bedding shear that disrupted a portion of the shaft. The pattern of shaft distortion is consistently measured by shaft instruments; this disruption is entirely consistent with shear induced by mining in the J vein. The sensitivity of displacement rate to geology is evident in the contrast between the MPBX displacement rates measured in sericitic quartzite (E1, E2, and E3) and the rates measured in siltite-argillite (E4), as well as shaft set distortion (figure 8). The influence of mining is evident in the incremental change in displacement rate caused by apparent activity in the Chester vein hanging wall and/or footwall. All data indicate that rock creep was consistently uniform, had a constant rate, and increased significantly toward the Chester vein and shaft, suggesting that the shaft structure was responding to long-term rock creep resulting from historic mining.

It is obvious that mining within even 30 m (100 ft) of the shaft will have (and has had) an effect on shaft stability. This pattern is evident in the structural models. However, the structural models do not include the various strata, and thus the local amplification of shaft distortion is not apparent. The computer modeling effort is a very simplified example of the effects of removing approximately 10,890 t (12,000 st) of ore, an amount approximating what was contained in the 4E and 4W blocks of the South Split of the Chester vein. The model indicates that typical rules of thumb, such as two-diameter zones of influence, are very difficult to apply when there are complex geometric configurations and variations in physical properties, such as is the case here.

The ability to create a mesh and analyze a very complex geometric network of openings in a deep mine was successfully accomplished through the use of submodeling. The application of CAD, automeshing, and submodeling has permitted significant progress to be made. Analyzing target areas is essential in mining because trouble spots and hazardous conditions are often highly localized, yet are affected by conditions well beyond the traditional zone of influence based on models of elastic or elastic-plastic material behavior. Although the behavior of large, highly stressed rock masses is poorly understood, the ability to define detailed areas of interest sequentially from a supermodel is an essential starting point.

The computer study produced displacement vectors, stress concentrations, and safety factors. Submodeling allowed target features, such as shaft sets, to be remodeled using results from a supermodel. These sets of instruments provided an extremely precise and long-term look at rock mass conditions that represents a significant advance in the ability to monitor rock mass behavior. The analysis demonstrates the critical role that structural geology plays in the development of rock mass deformation. Results are being used to design new approaches to mine design and shaft monitoring and to provide design guidelines for deep mine accessways subject to very large rock-mass-loading conditions.

ACKNOWLEDGMENTS

The authors express their gratitude to officials and personnel of Sunshine Mining Co., particularly John Jordan, chief engineer, Tom Fudge, mine superintendent, and Jerry Hollis, engineering technician, who provided access to the mine, equipment and services, and assistance with reading the instruments. Special thinks go to William Hand, electrical technician, retired, Spokane Research Center, who assembled the DAS and sensor array and installed the instruments at the test site.

REFERENCES

1. Beus, M. J., and M. P. Board. Field Measurement of Rock Displacement and Support Pressure at 5955-ft Level During Sinking of a Deep Circular Shaft in Northern Idaho. USBM RI 8909, 1984, 11 pp.

2. Beus, M. J., and S. M. Dar. Three-Dimensional FEM Analysis To Scale Field Measurements from Deep Mine Accessways. Paper in Rock Mechanics as a Guide for Efficient Utilization of Natural Resources: Proceedings of the 30th U.S. Symposium on Rock Mechanics, ed. by A. W. Khair (WV Univ., Morgantown, WV, June 19-22, 1989). Balkema, 1989, pp. 783-790.

3. Whyatt, J. K., and M. J. Beus. In Situ Stress at the Lucky Friday Mine (In Four Parts): 1. Reanalysis of Overcore Measurements From 4250 Level. USBM RI 9532, 1995, 26 pp.

4. Pariseau, W. G., J. C. Johnson, and S. A. Orr. Three-Dimensional Analysis of a Shaft Pillar at the Homestake Mine. Paper in Rock Mechanics Contributions and Challenges: Proceedings of the 31st U.S. Symposium on Rock Mechanics, ed. by W. A. Hustrulid and G. A. Johnson (CO Sch. Mines, Golden, CO, June 18-20, 1990). Balkema, 1990, pp. 529-536.

5. Bruce, M. F. G., and A. W. Stilwell. Shaft Pillar Removal in an Operating Shaft. Paper in International Deep Mining Conference: Technical Challenges in Deep Level Mining, ed. by D. A. J. Ross-Watt and P. D. K. Robinson (Johannesburg, S. Afr., Sept. 17-21, 1990). S. Afr. Inst. Min. and Metall., Johannesburg, S. Afr., 1990, pp. 681-699.

6. Solms, R. L. Mine Design with Special Reference to Shaft Pillars at Great Depths. Paper in Mining, ed. by J. T. Brady, R. L. Kay, and I. L. Hore-Lacy (Proc., 13th CMMI Cong., May 11-16, 1986, Singapore). V. 3, 13th Congr. Coun. Min. and Metall. Inst., 1986, pp. 21-29.

7. Leach, A. R. Early Shaft Reef Extraction-The Western Deep Levels South Approach to Shaft Protection. Paper in Static and Dynamic Considerations in Rock Engineering. Balkema, 1990, pp. 183-195.

8. Willewse, R. B. Reef Extraction of a Shaft Pillar at Western Deep Levels Limited. Paper in International Deep Mining Conference: Technical Challenges in Deep Level Mining, ed. by D. A. J. Ross-Watt and P. D. K. Robinson (Johannesburg, S. Afr., Sept. 17-21, 1990). S. Afr. Inst. Min. and Metall., Johannesburg, S. Afr., 1990, pp. 659-670.

9. Whyatt, J. K., and E. L. Hardin. Microcomputer-Based Instrumentation System for Monitoring Ground Support in a Deep Mine Shaft. USBM IC 9062, 1986, 88 pp.

10. Micro Specialties System (Bath, PA). RTM 3500-Real Time Multitasking Data Acquisition Package, Ver. 2.10. 1987, 25 pp.

11. Desalvo, G. J., and R. W. Gorman. ANSYS User's Manual, Rev. 4.4. Swanson Analysis Systems, Houston, PA, 1989, 364 pp.

Figure 1

Collapse of shaft support structure that could have resulted from instability in rock mass.

Figure 2

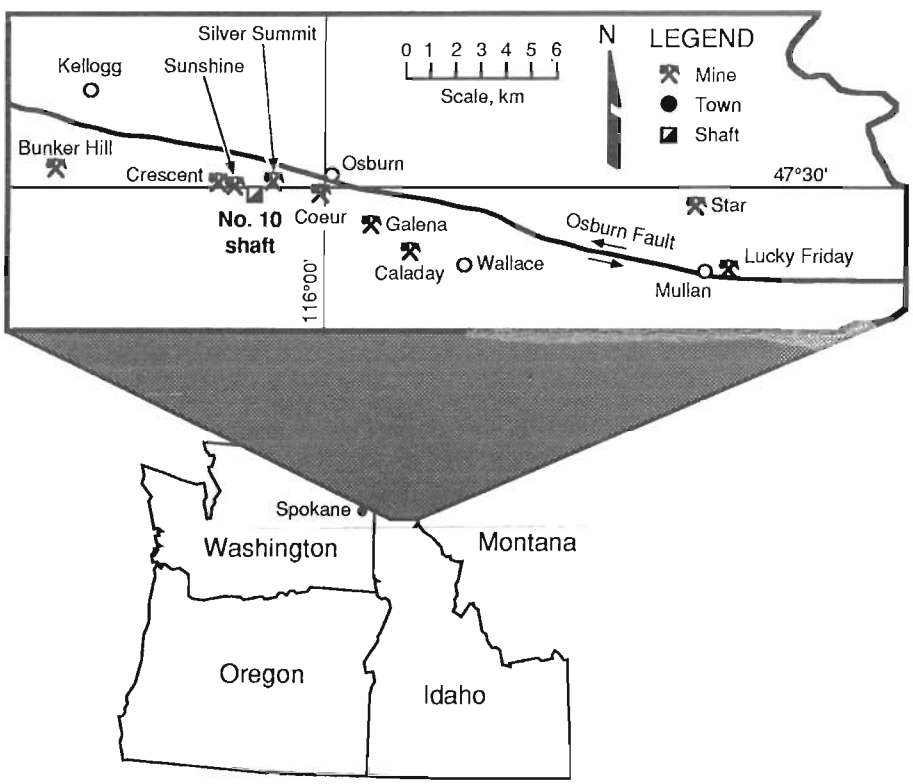

Location of shaft at Sunshine Mine.

Figure 3

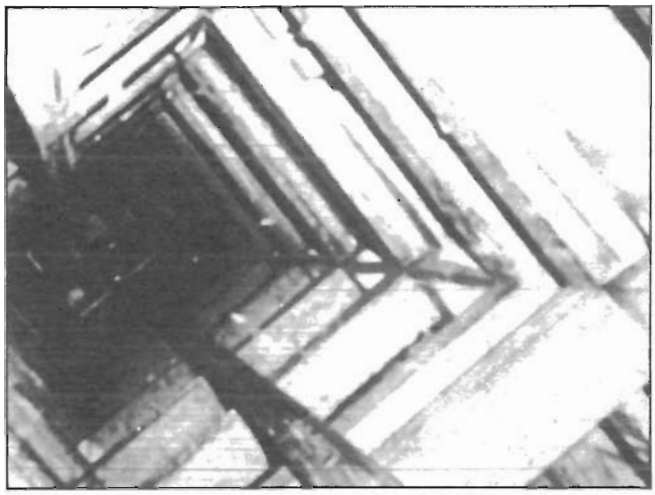

Guides and shaft sets in chippy compartment of shaft.

Figure 4

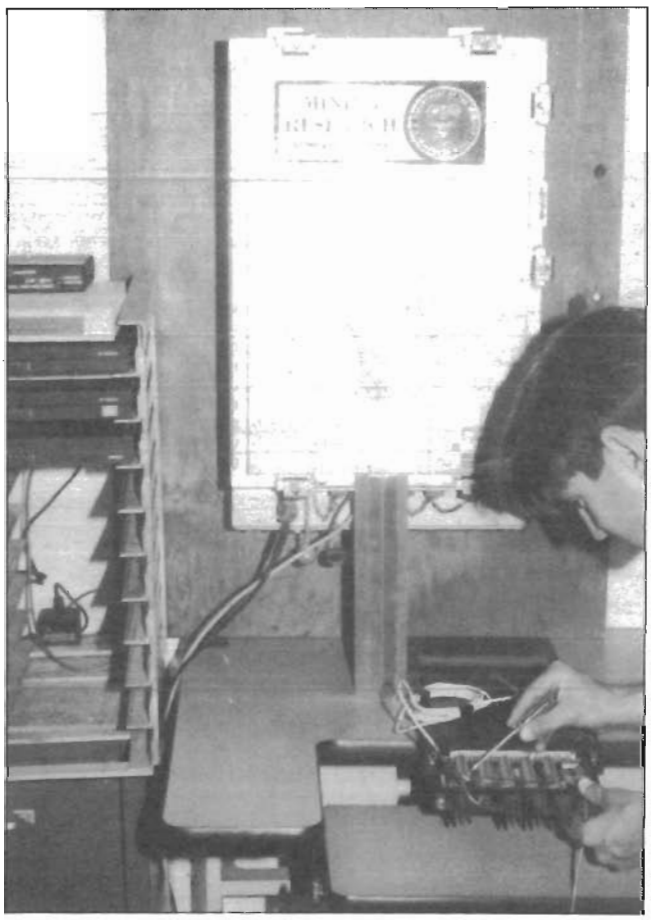

Present configuration of passive backplane system with board-level 486 processor.

Figure 5

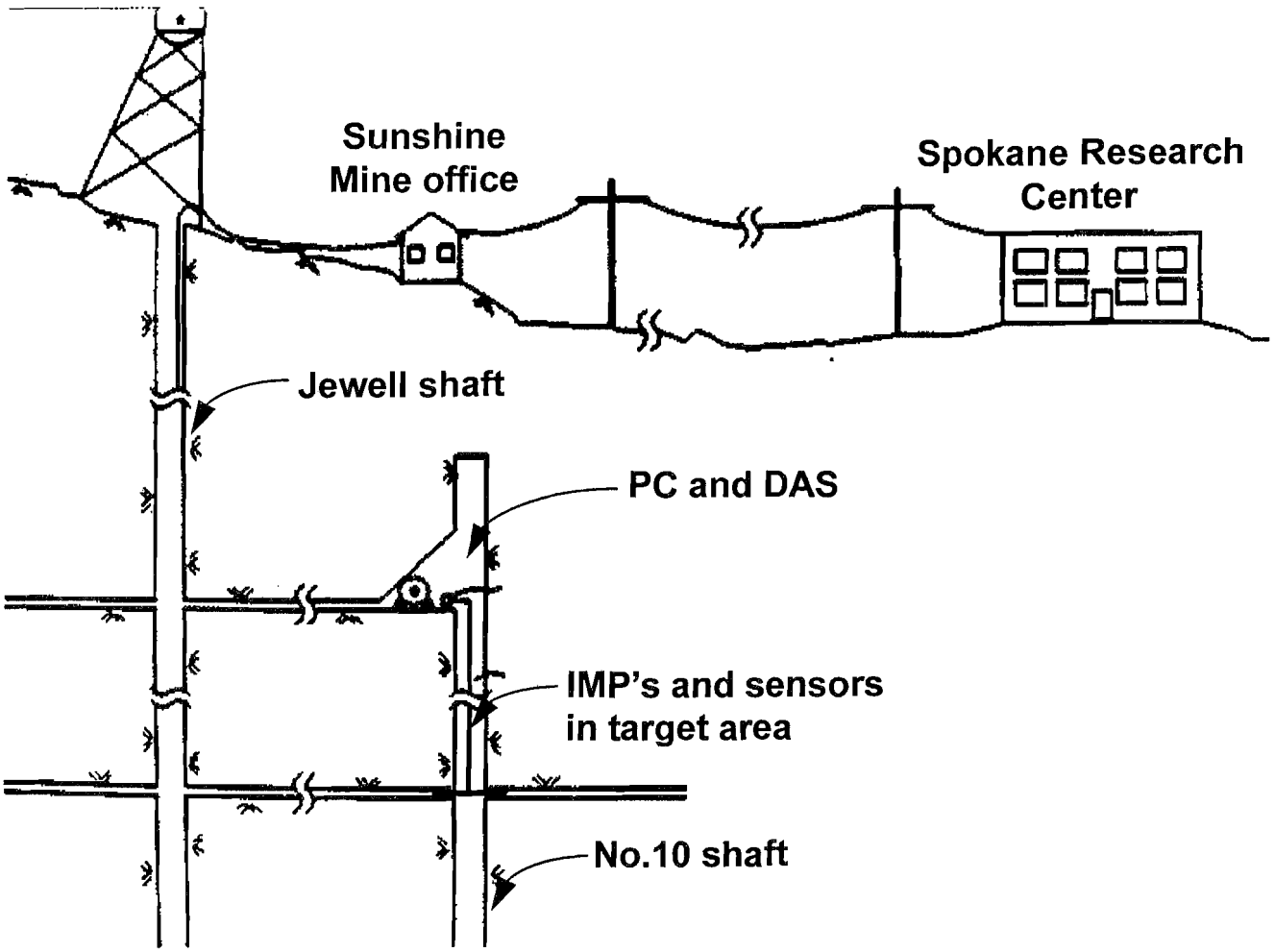

Experimental layout at Sunshine Mine.

Figure 6

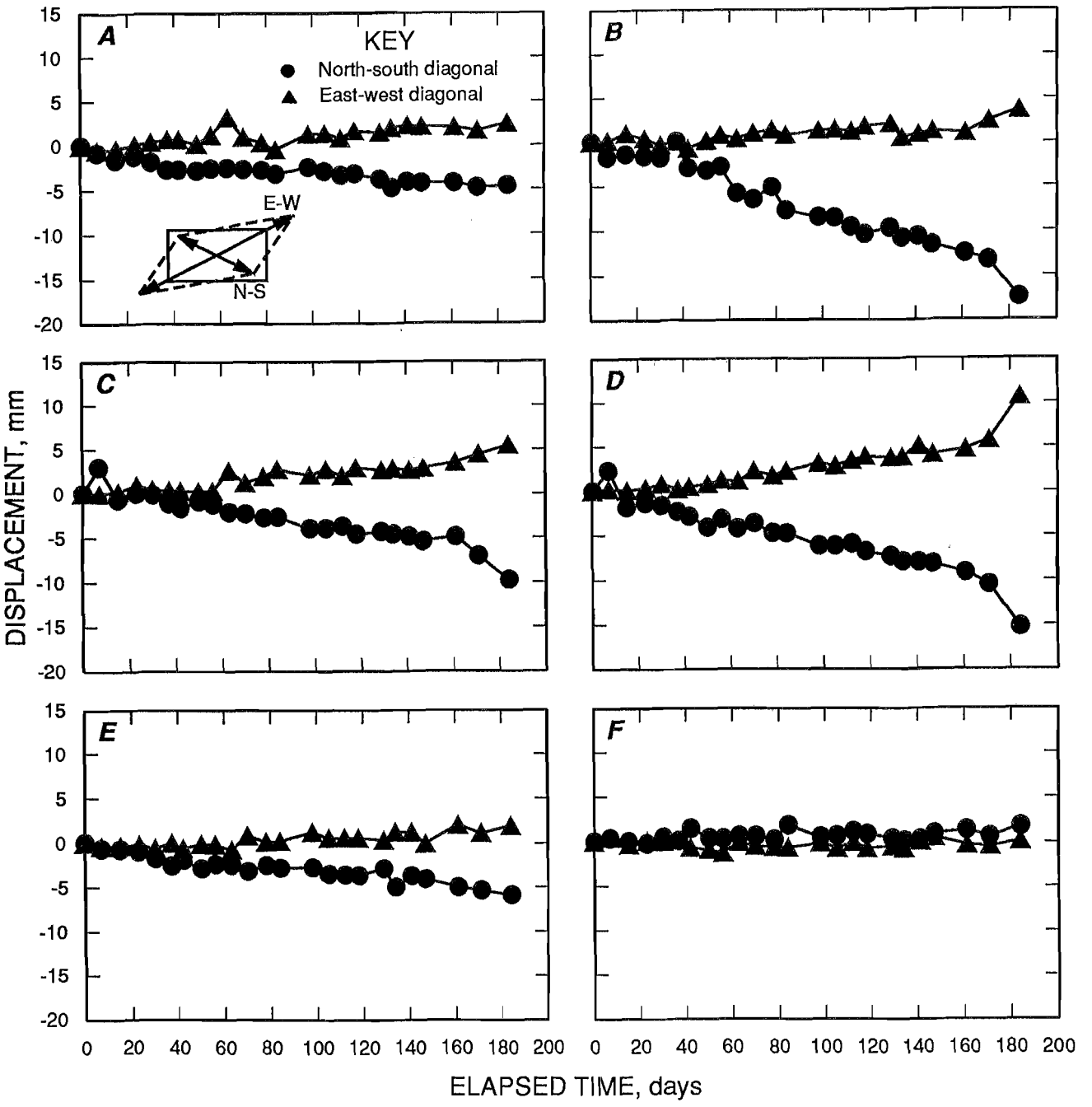

Diagonal distortion in shaft support sets. A, Set 40-16; B, set 42-09; C, set 42-14; D, set 42-30; E, set 44-13; F, set 46-15.

Figure 7

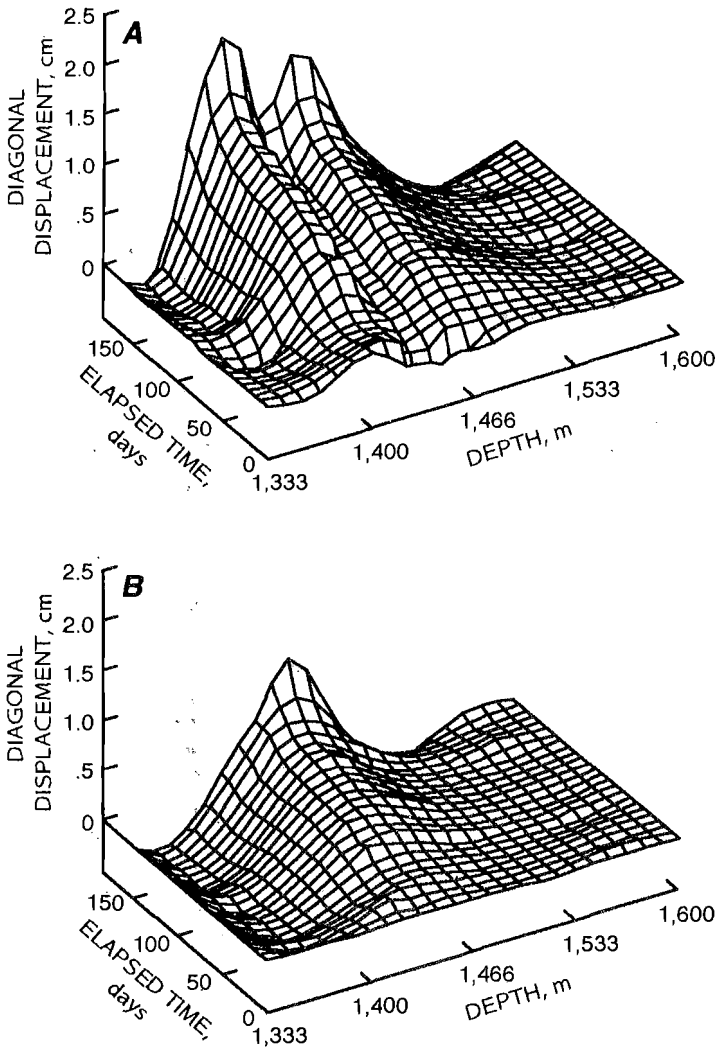

Three-dimensional plots of absolute values of diagonal displacements. A, North-south diagonals; B, east-west diagonals.

Figure 8

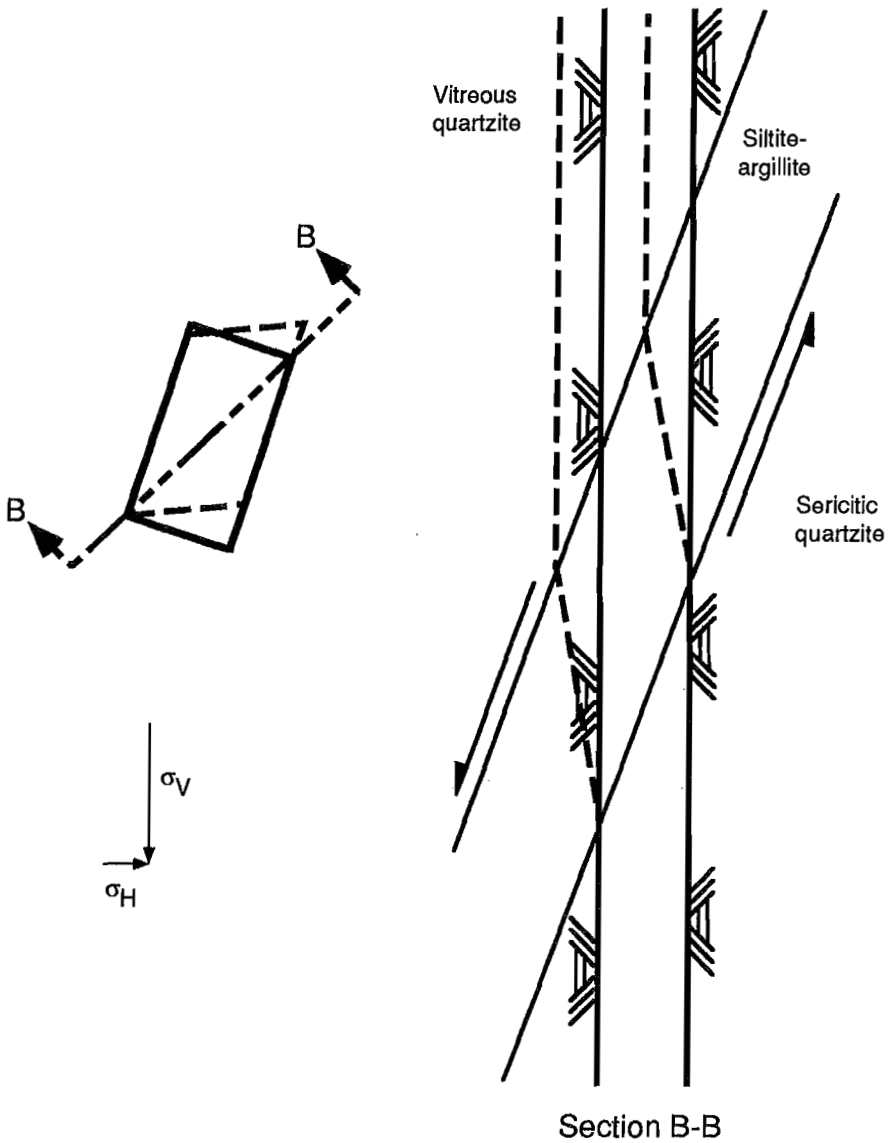

East-west section (B-B) in No. 10 shaft showing possible shear mechanisms and resulting distortion (dotted line). σ_H ***= horizontal stress and*** σ_V ***= vertical stress.***

Figure 9.

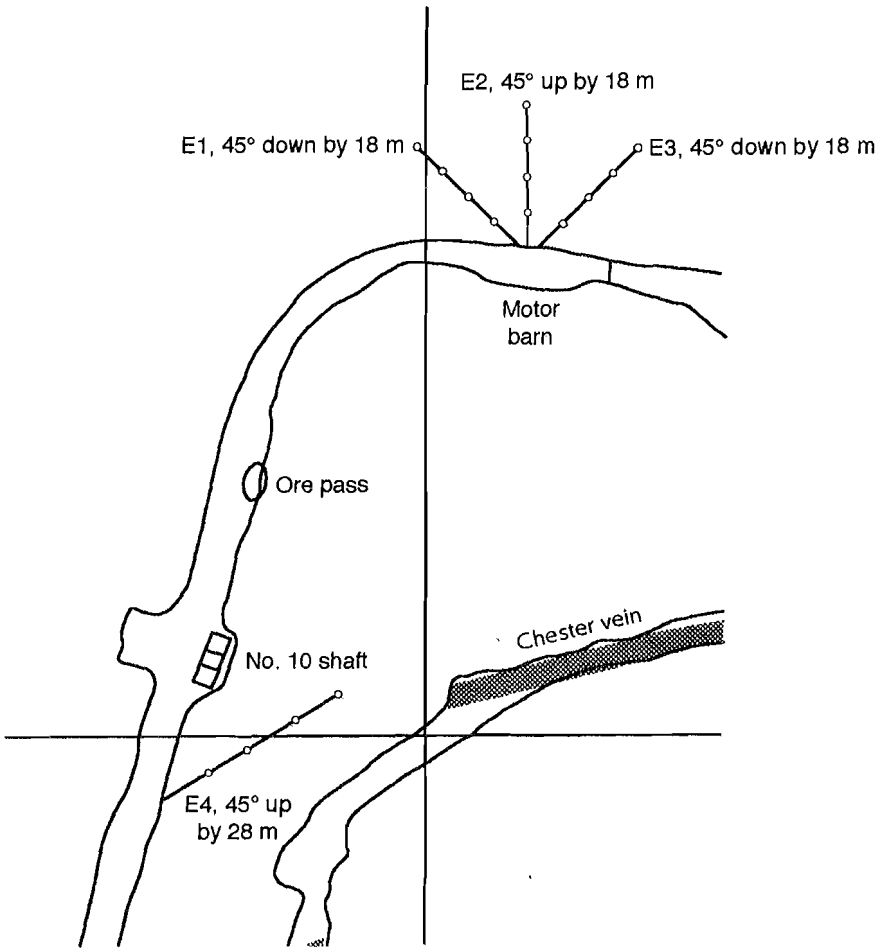

Instrument layout and MPBX location on 4400 level.

Figure 10

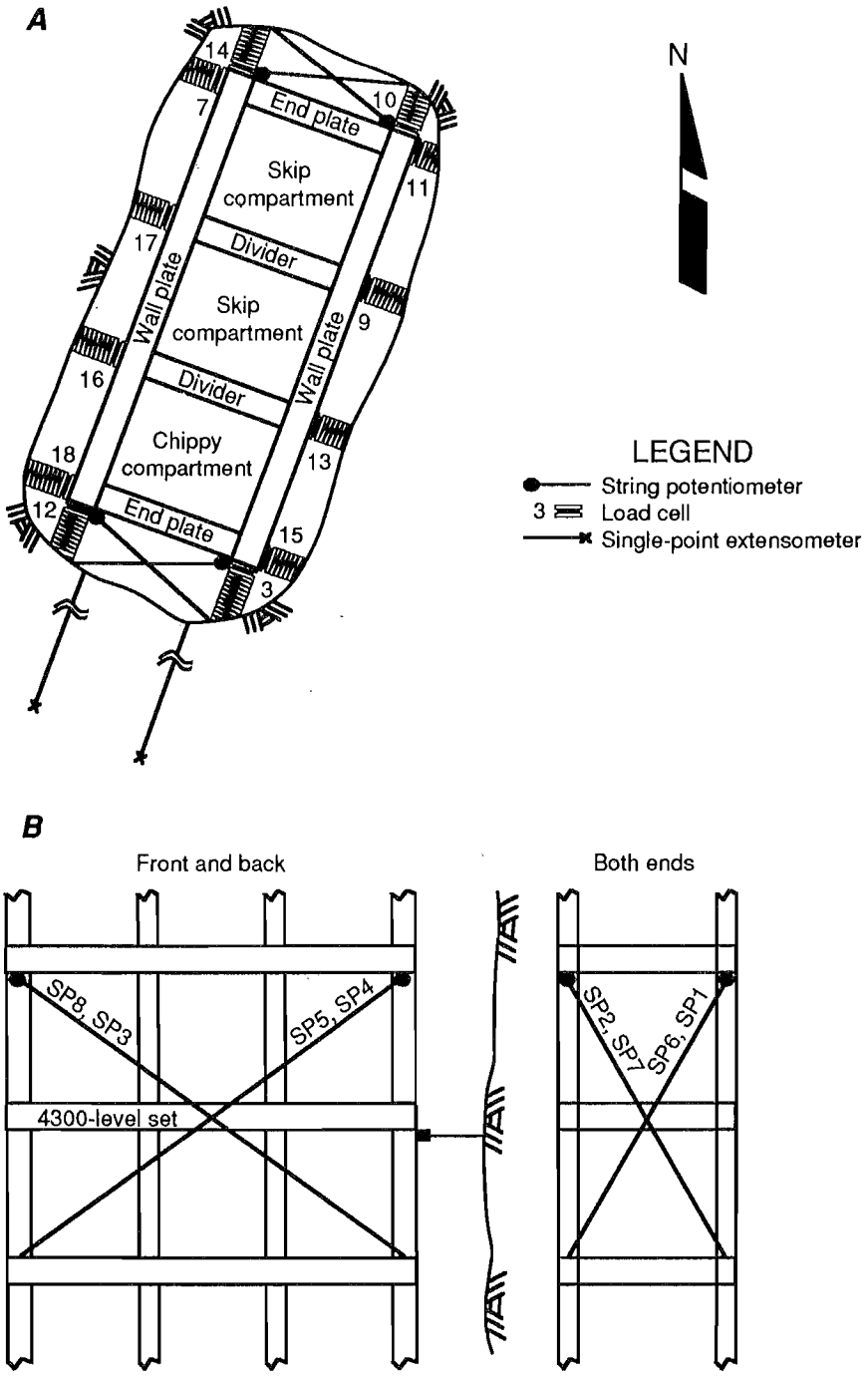

Locations of shaft monitoring instruments. A, Load cells; B, string potentiometers.

Figure 11

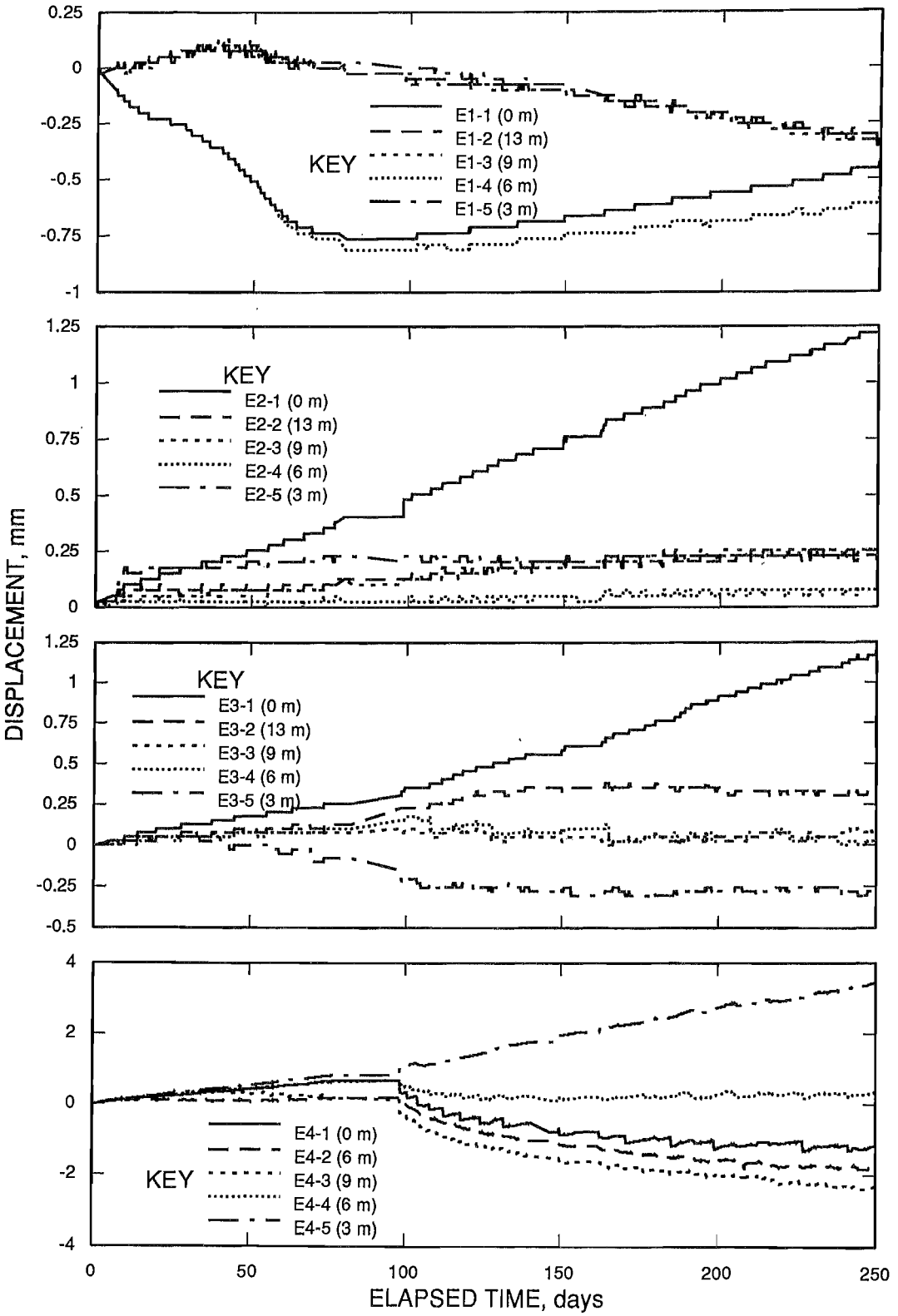

MPBX plots of displacements on 4400 level.

Figure 12

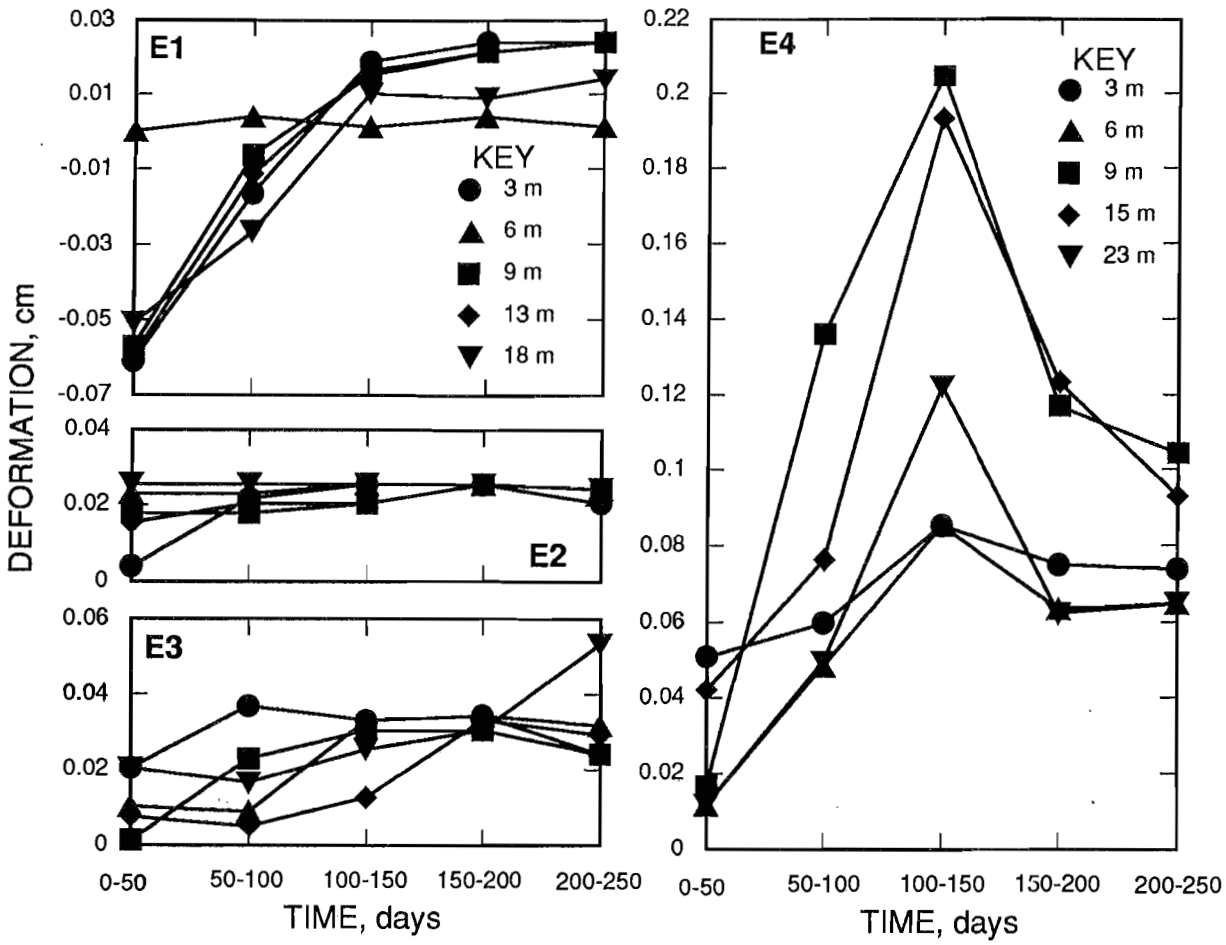

Incremental displacements indicated by MPBX's over successive 50-day monitoring periods.

Figure 13

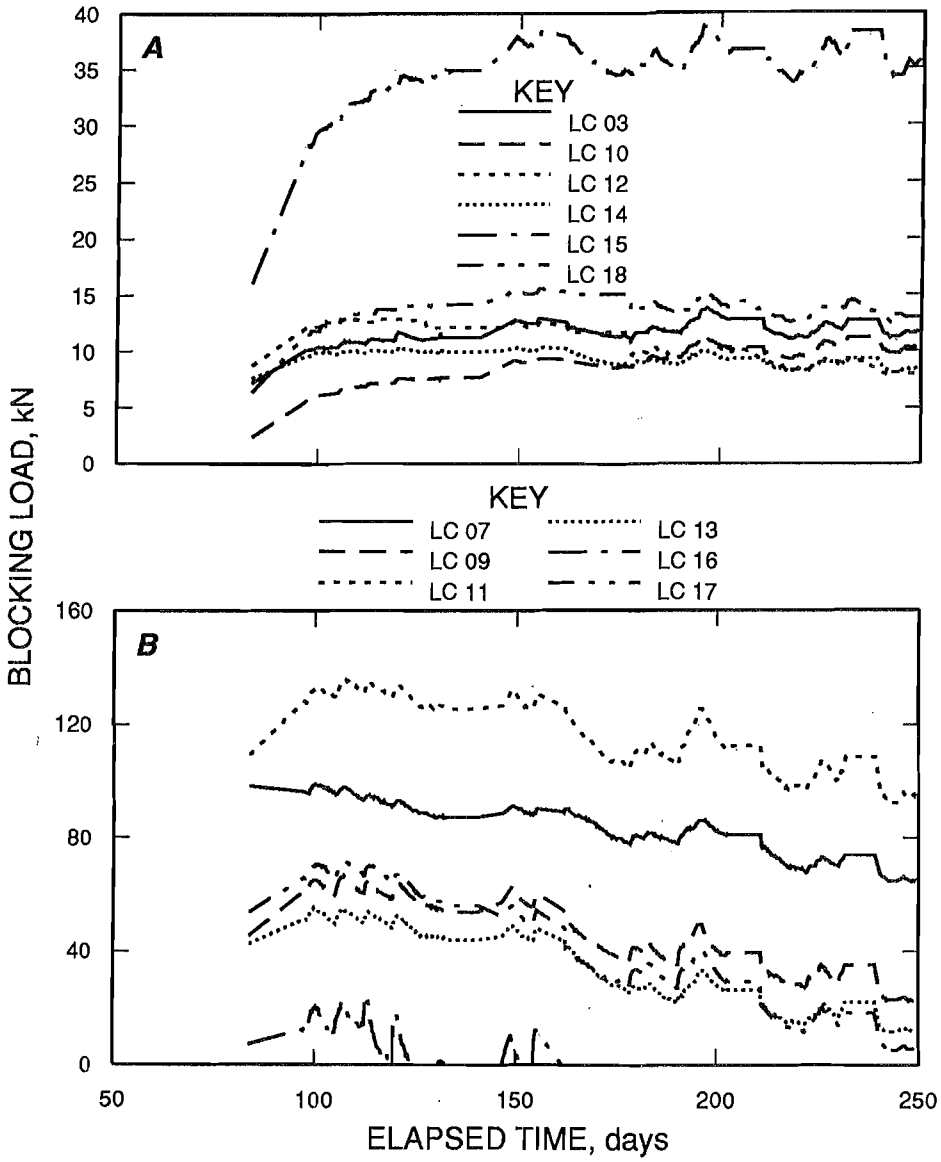

LC plots from timber set at 4300 level. A, Loads on wall end plates; B, loads across compartment dividers.

Figure 14

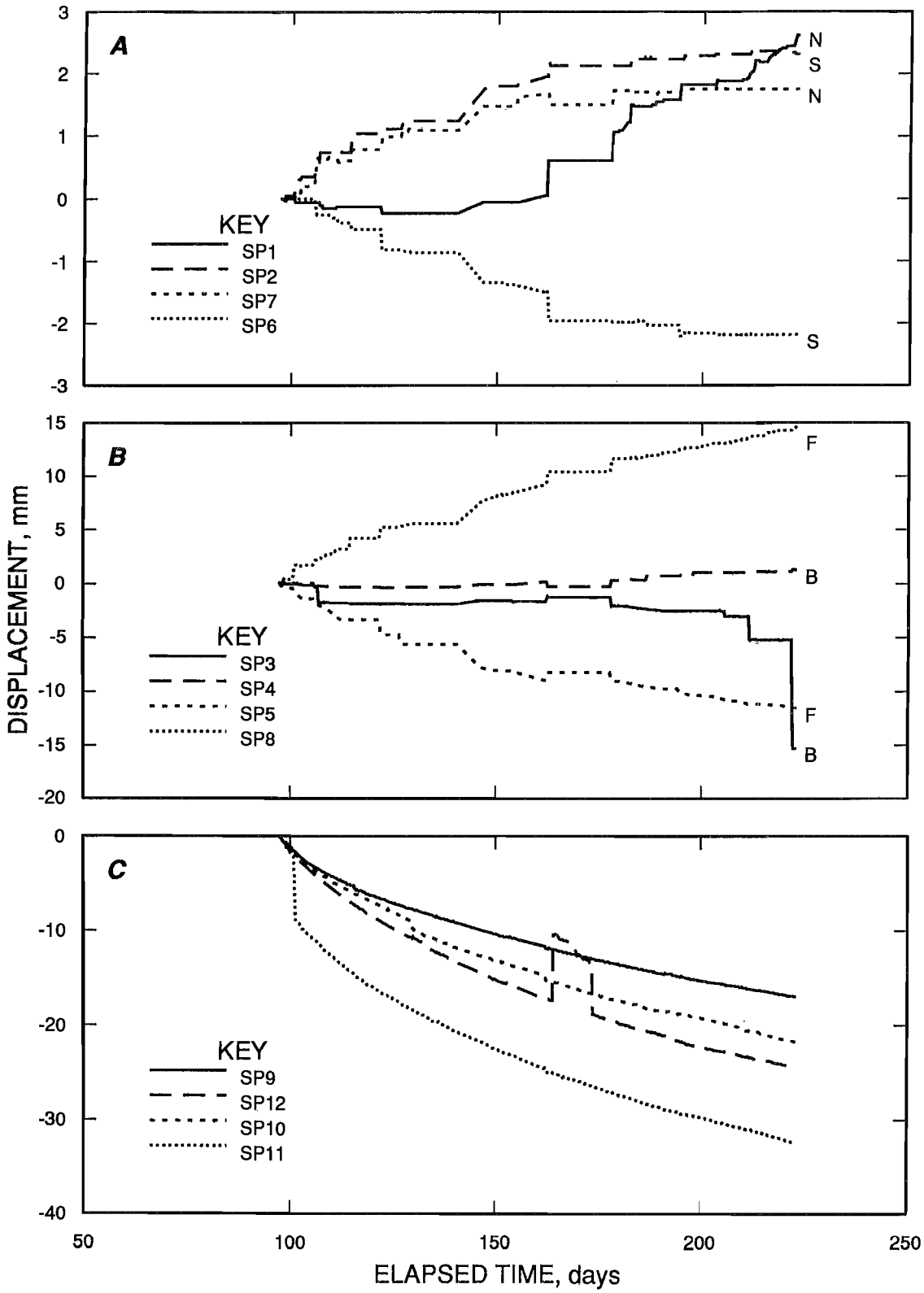

Diagonal distortion of three shaft sets centered around 4300 level. A, North and south end; B, front of shaft; C, short diagonals on south end of shaft at center shaft set.

Figure 15

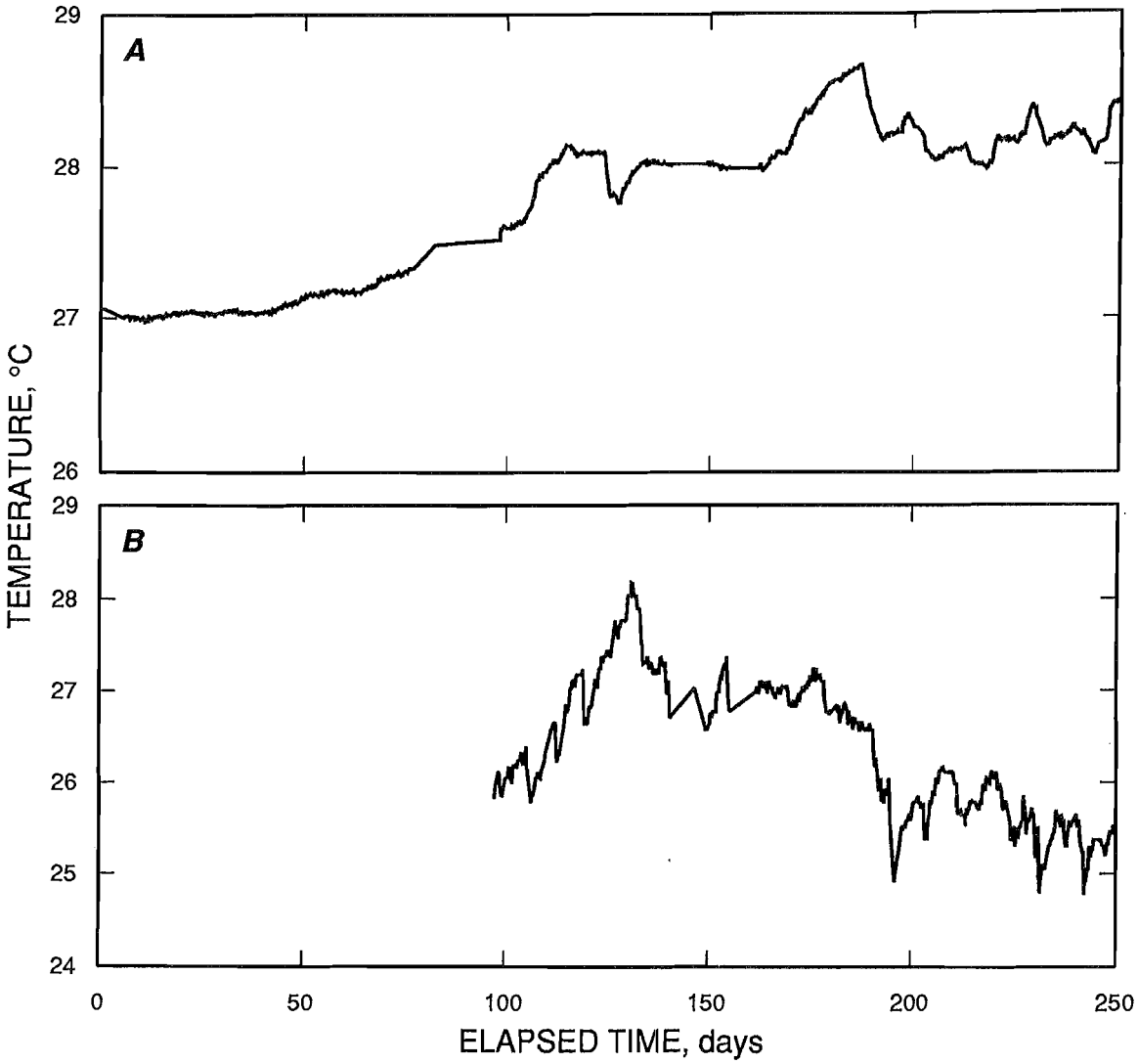

Temperatures at (A) MPBX E1 on 4400-level drift and (B) inside chippy compartment.

Figure 16

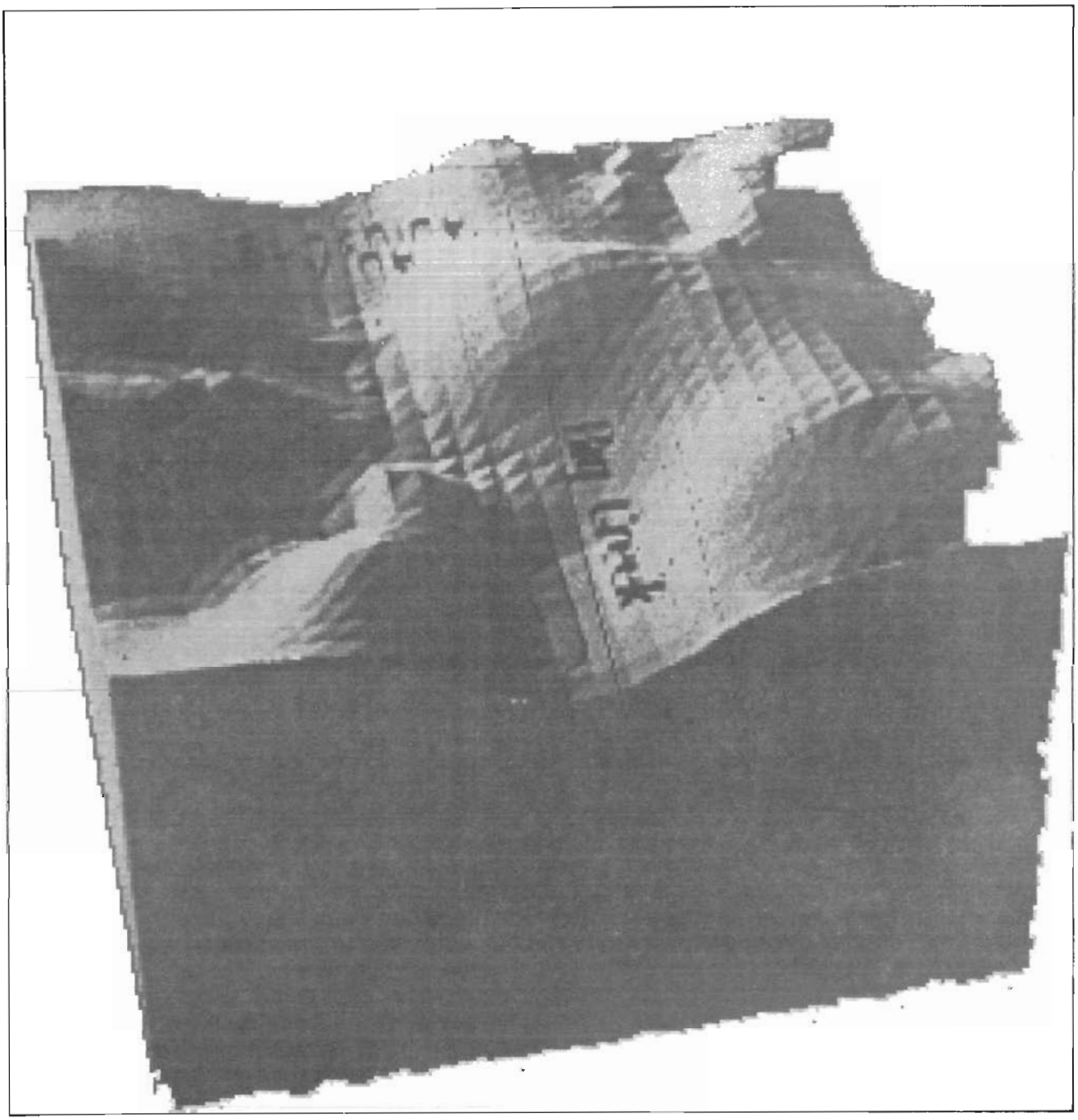

Computerized rendition of topography of Sunshine Mine area.

Figure 17

Vertical stress distribution on horizontal slice at 4400 level for 1-km² area centered around No. 10 shaft.

Figure 18

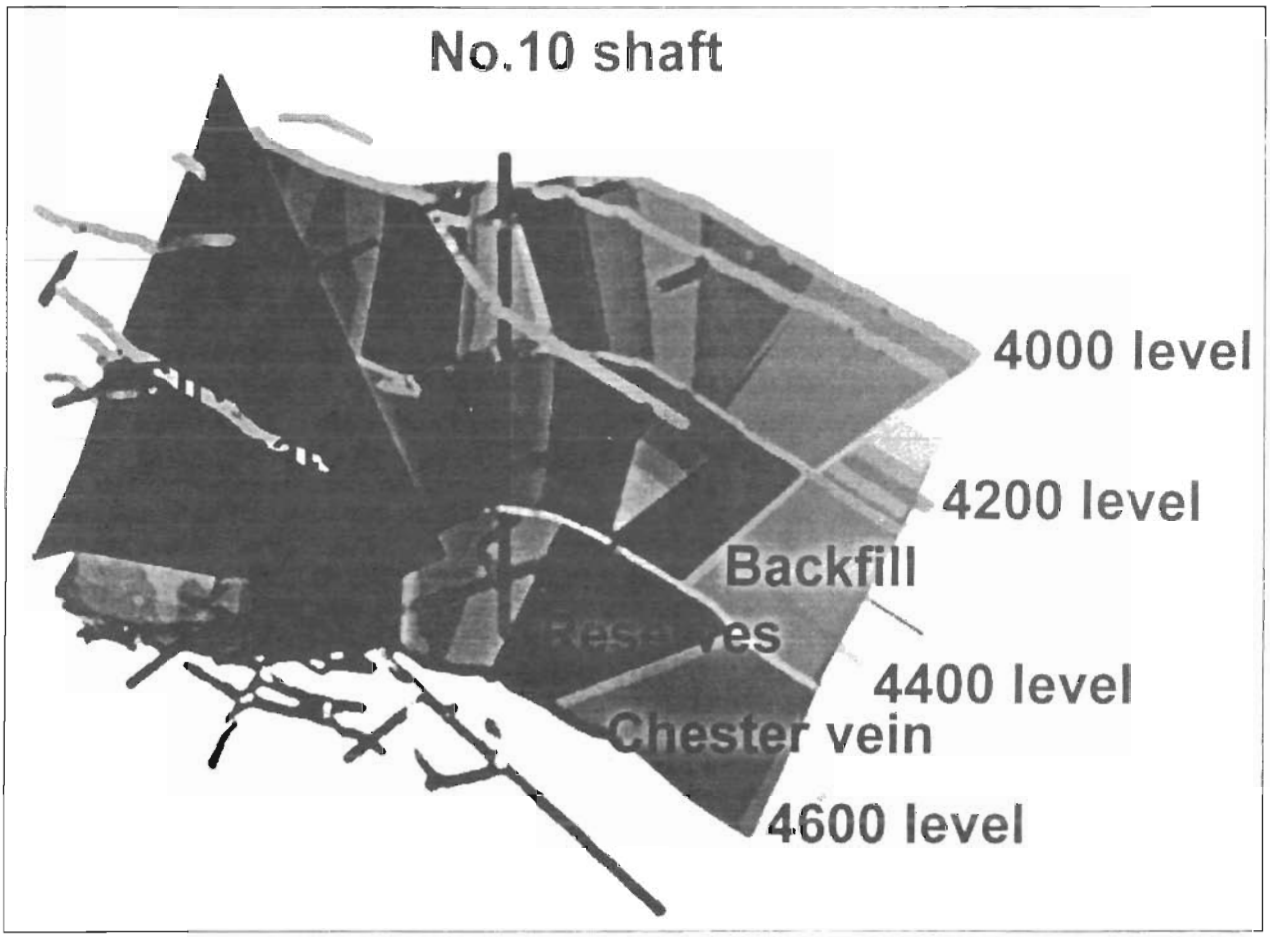

Ore deposits, mined and backfilled areas, reserves, and major geologic features.

Figure 19

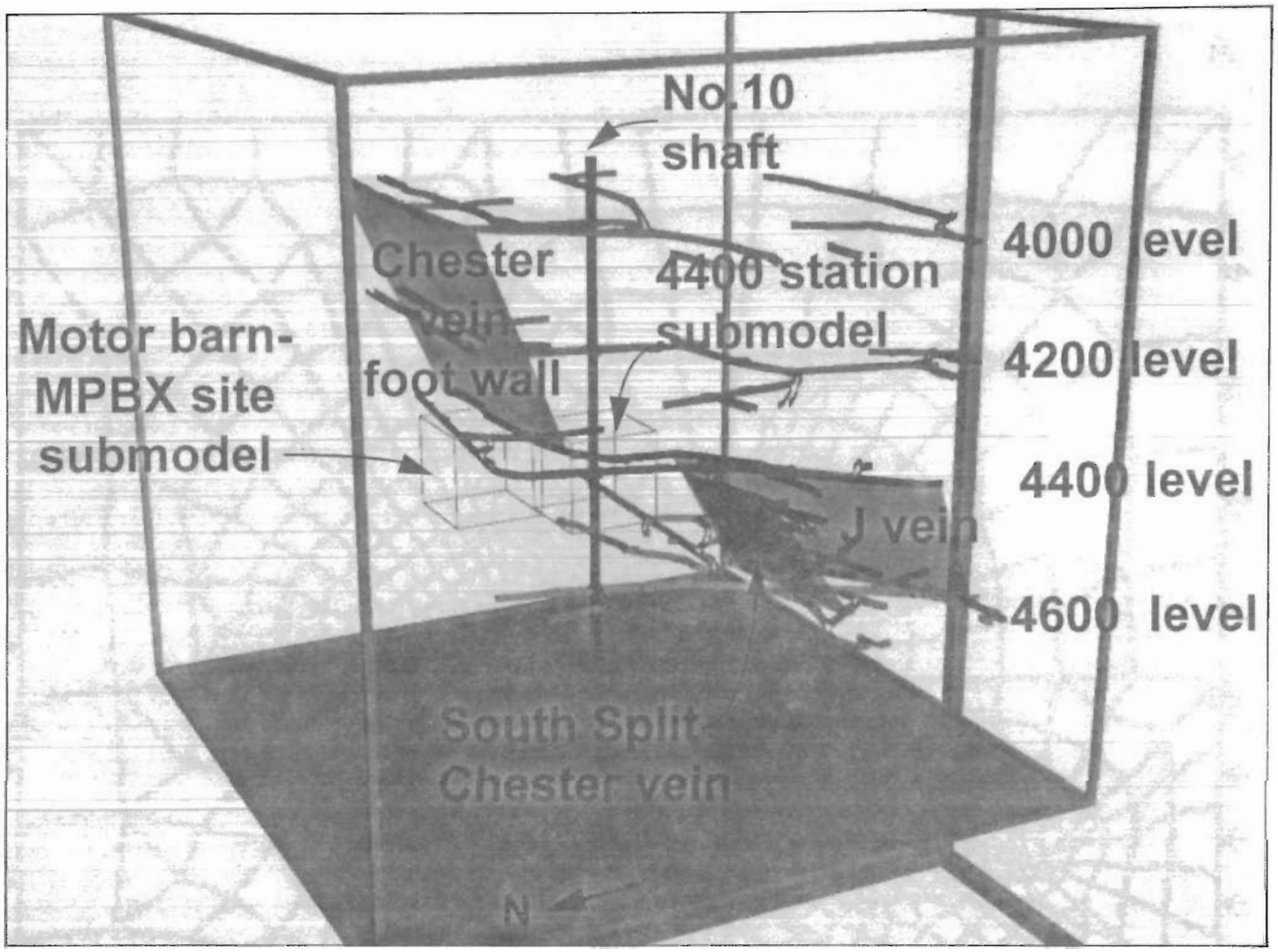

Gross vein submodel with motor barn and 4400 station submodels.

Figure 20

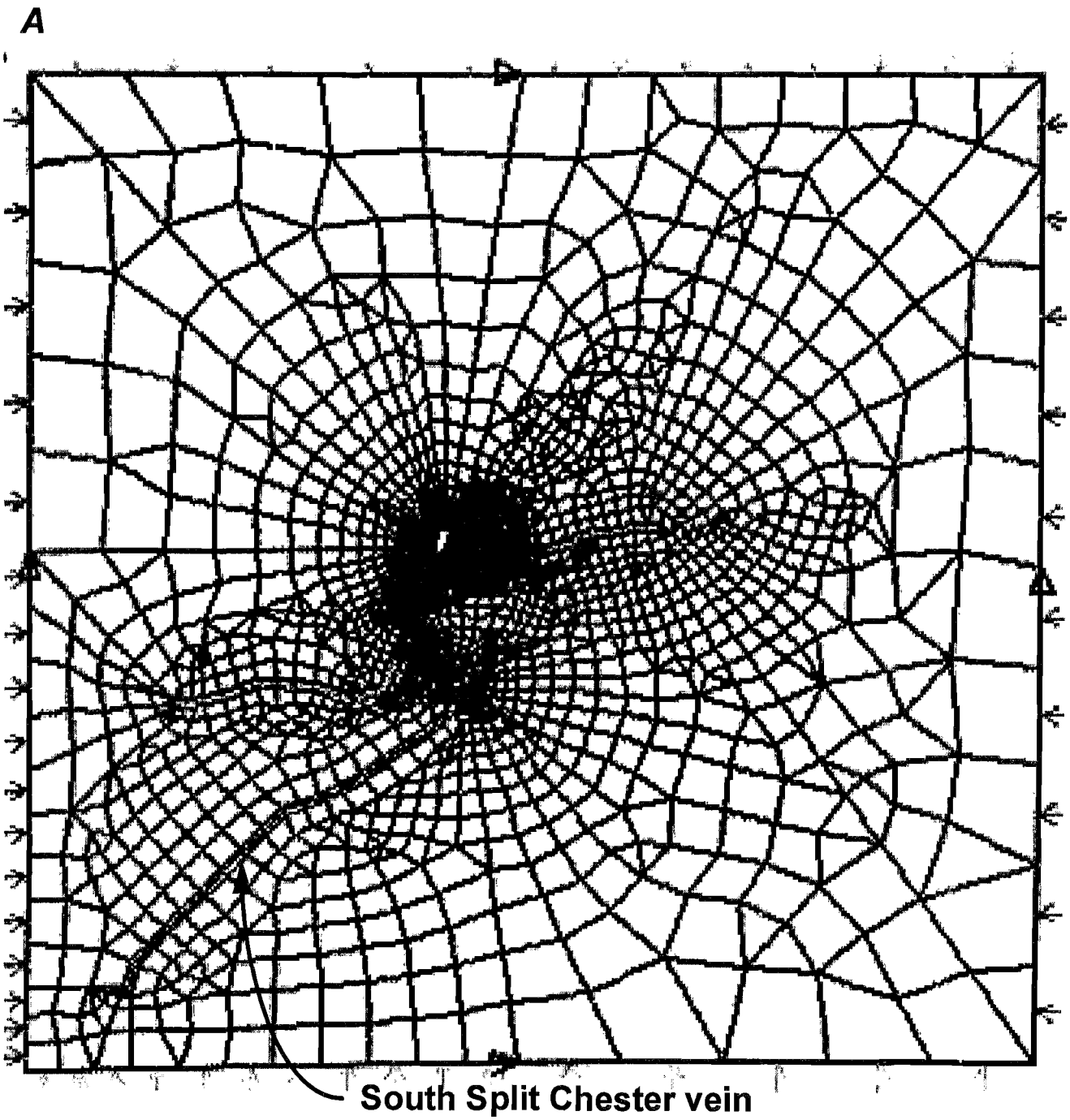

Two-dimensional cross-section mesh developed to show veins in relation to No. 10 shaft. A, South Split vein of Chester vein.

Figure 20—Continued

B

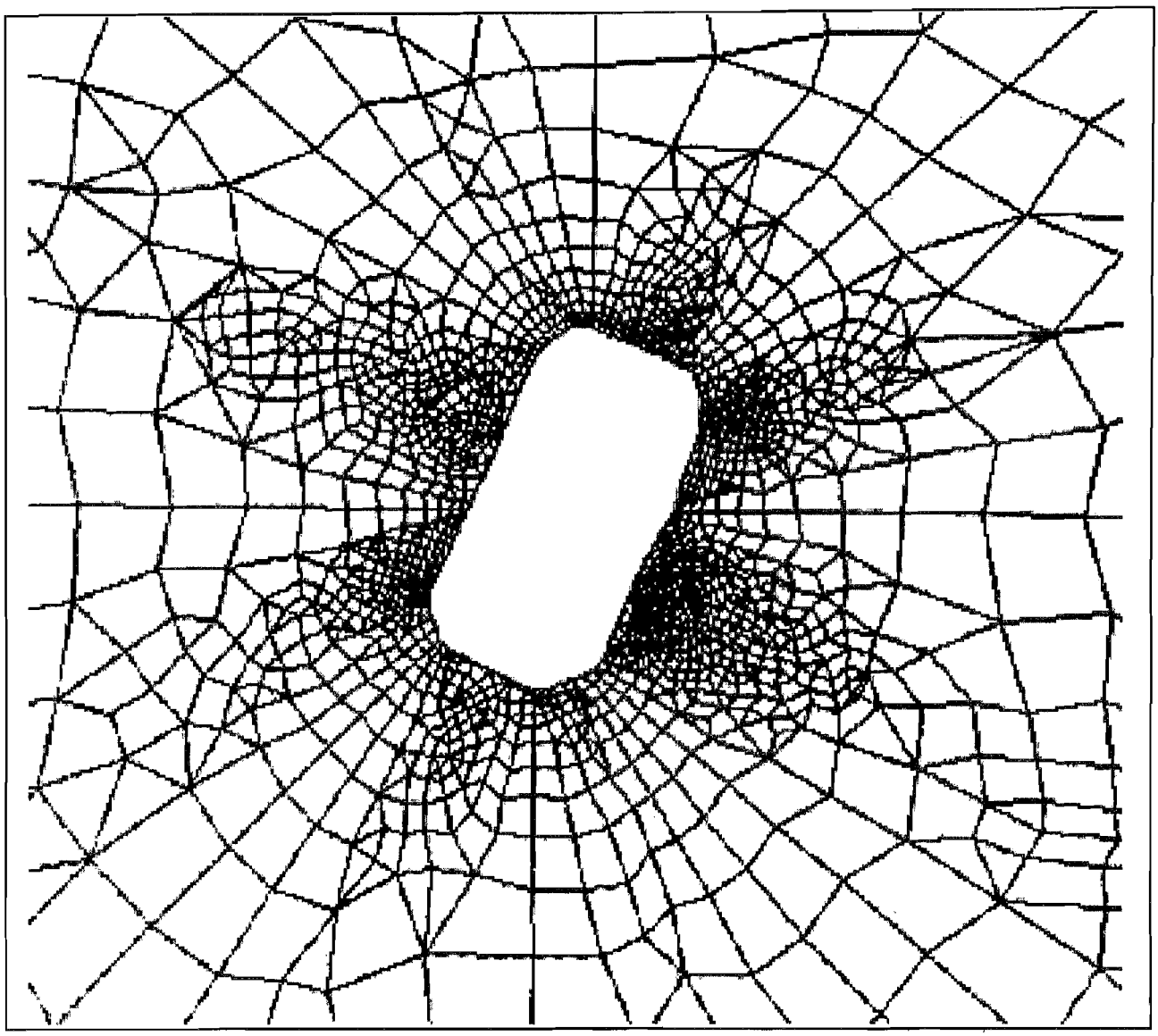

B, mesh in which shaft opening is treated as rectangular rock section.

Figure 20—Continued

C

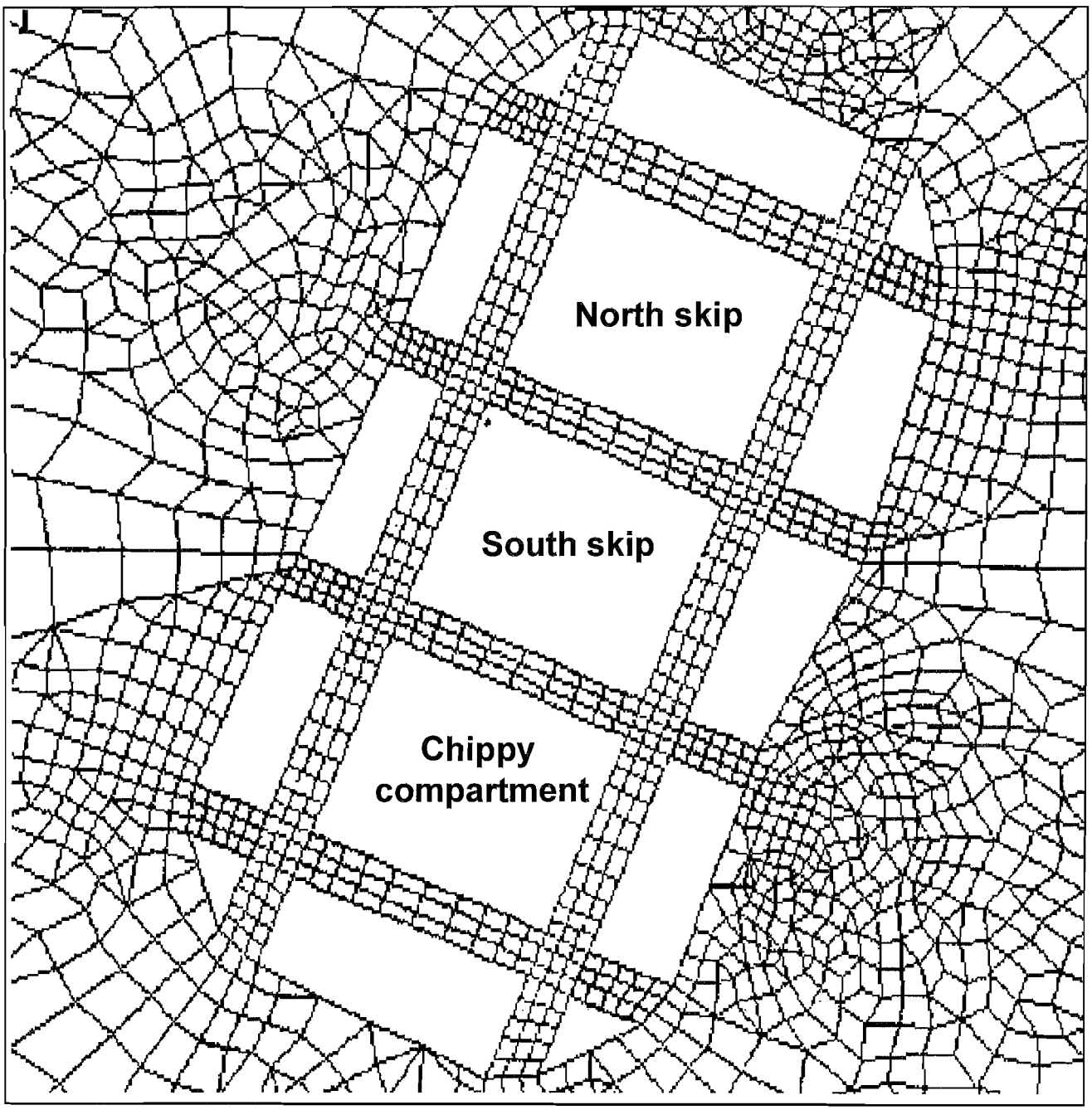

C, shaft set mesh at 4300 level.

Figure 21

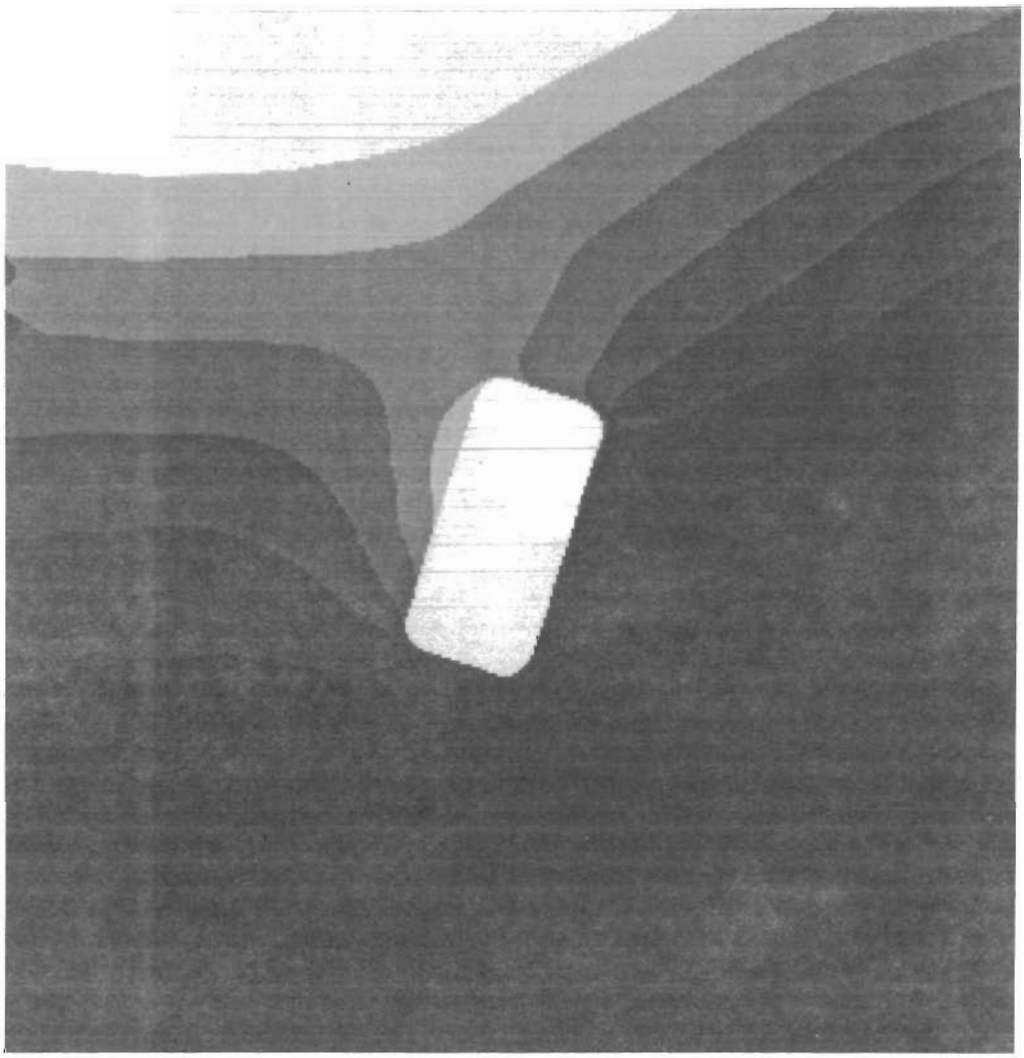

Relative difference in vertical deformation between northwest and southeast corners of shaft opening. Darker shades indicate greater movement or stress.

Figure 22

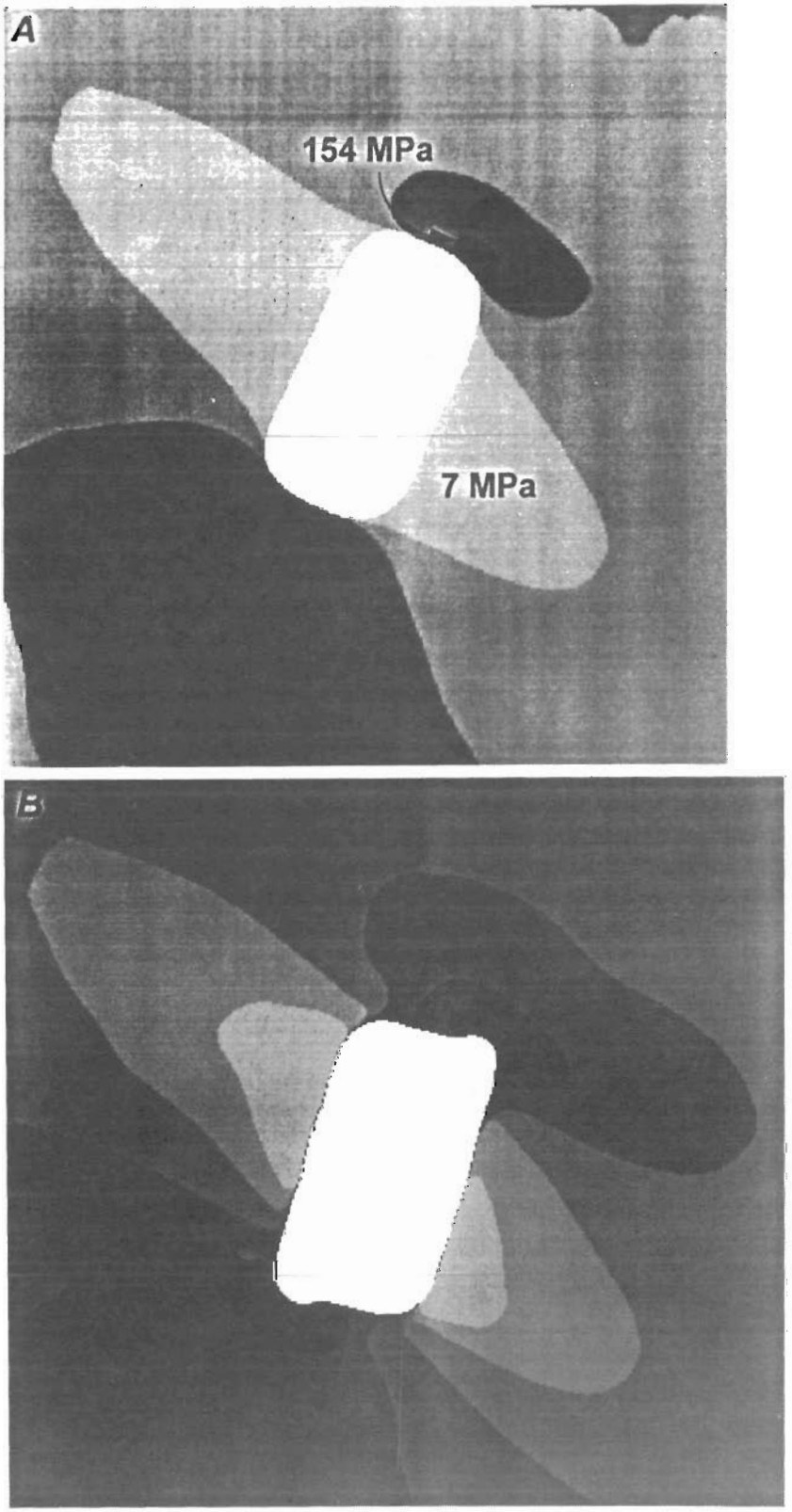

Maximum stress surrounding shaft section. A, Before mining; B, after mining.

Figure 23

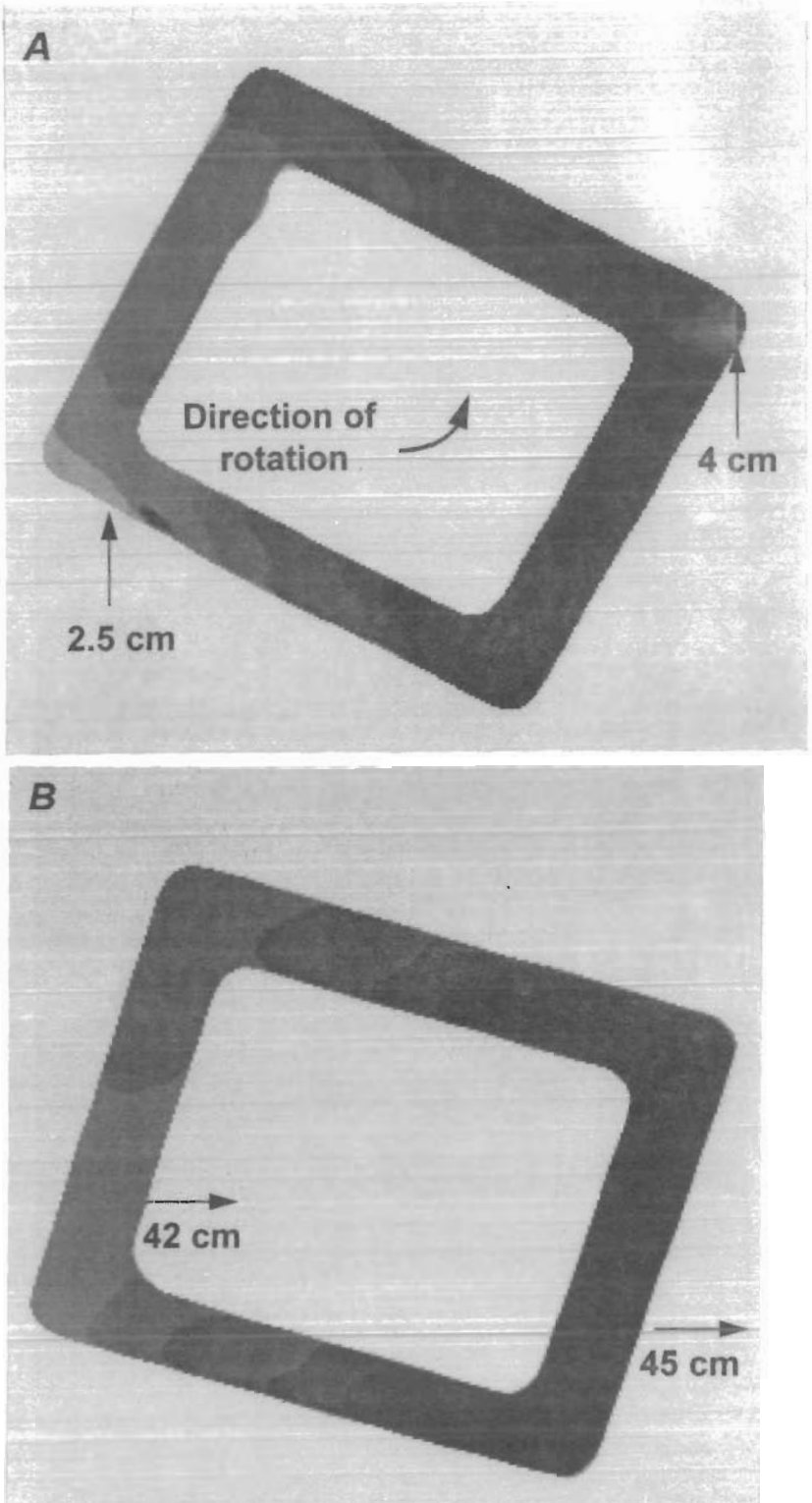

Rotational trend and translation in shaft support set. A, North-south movement indicating translation toward north; B, east-west movement indicating lengthening of east-west axis and extensive translation toward the east.

INT.BU.OF MINES,PGH.,PA 30213
☆ USGPO 709-137/20,073